

Asymmetrically interacting spreading dynamics on complex layered networks

Wei Wang,¹ Ming Tang,^{1,2,*} Hui Yang,¹ Younghae Do,³ Ying-Cheng Lai,⁴ and GyuWon Lee⁵

¹*Web Sciences Center, University of Electronic Science and Technology of China, Chengdu 610054, China*

²*Center for Atmospheric Remote Sensing(CARE), Kyungpook National University, Daegu, 702-701, South Korea*

³*Department of Mathematics, Kyungpook National University, Daegu 702-701, South Korea*

⁴*School of Electrical, Computer and Energy Engineering,
Arizona State University, Tempe, Arizona 85287, USA*

⁵*Department of Astronomy and Atmospheric Sciences, Center for Atmospheric Remote Sensing(CARE),
Kyungpook National University, Daegu, 702-701, South Korea*

(Dated: May 9, 2014)

The spread of disease through a physical-contact network and the spread of information about the disease on a communication network are two intimately related dynamical processes. We investigate the asymmetrical interplay between the two types of spreading dynamics, each occurring on its own layer, by focusing on the two fundamental quantities underlying any spreading process: epidemic threshold and the final infection ratio. We find that an epidemic outbreak on the contact layer can induce an outbreak on the communication layer, and information spreading can effectively raise the epidemic threshold. When structural correlation exists between the two layers, the information threshold remains unchanged but the epidemic threshold can be enhanced, making the contact layer more resilient to epidemic outbreak. We develop a physical theory to understand the intricate interplay between the two types of spreading dynamics.

Epidemic spreading [1–6] and information diffusion [7–10] are two fundamental types of dynamical processes on complex networks. While traditionally these processes have been studied independently, in real-world situations there is always coupling or interaction between them. For example, whether large-scale outbreak of a disease can actually occur depends on the spread of information about the disease. In particular, when the disease begins to spread initially, individuals can become aware of the occurrence of the disease in their neighborhoods and consequently take preventive measures to protect themselves. As a result, the extent of the disease spreading can be significantly reduced [11–13]. A recent example is the wide spread of severe acute respiratory syndrome (SARS) in China in 2003, where many people took simple but effective preventive measures (e.g., by wearing face masks or staying at home) after becoming aware of the disease, even before it has reached their neighborhoods [14]. To understand how information spreading can mitigate epidemic outbreaks, and more broadly, the interplay between the two types of spreading dynamics has led to a new direction of research in complex network science [15].

A pioneering step in this direction was taken by Funk *et al.*, who presented an epidemiological model that takes into account the spread of awareness about the disease [16, 17]. Due to information diffusion, in a well-mixed population, the size of the epidemic outbreak can be reduced markedly. However, the epidemic threshold can be enhanced only when the awareness is sufficiently strong so as to modify the key parameters associated with the spreading dynamics such as the infection and recovery rates. A reasonable setting to investigate the complicated interplay between epidemic spreading and information diffusion is to assume two interacting network layers of identical set of nodes, one for each type of spreading dynamics. Due to the difference in the epidemic and information spreading processes, the connection patterns in the two layers can in general be quite distinct. For the special case where the two-layer overlay networks are highly correlated in the sense that they have completely overlapping links and high clustering coefficient, a locally spreading awareness triggered by the disease spreading can raise the threshold even when the parameters in the epidemic spreading dynamics remain unchanged [16, 17]. The situation where the two processes spread successively on overlay networks was studied with the finding that the outbreak of information diffusion can constrain the epidemic spreading process [18]. An analytical approach was developed to provide insights into the symmetric interplay between the two types of spreading dynamics on layered networks [19]. A model of competing epidemic spreading over completely overlapping networks was also proposed and investigated, revealing a coexistence regime in which both types of spreading can infect a substantial fraction of the network [20].

While the effect of information diffusion (or awareness) on epidemic spreading has attracted much recent interest [21–28], many outstanding issues remain. In this paper we address the following three issues. The first concerns the network structures that support the two types of spreading dynamics, which were assumed to be identical in some existing works. However, in reality, the two networks can differ significantly in their structures. For example, in a modern society, information is often transmitted through electronic communication networks such as telephones [29] and the Internet [30], but disease spreading usually takes place on a physical contact network [31]. The whole complex system should then be modeled as a double-layer coupled network (overlay network or multiplex network) [32–36], where each layer has a distinct internal structure and the interplay between the two layers has diverse characteristics, such as inter-similarity [37], multiple support dependence [38], and inter degree-degree correlation [39], etc. The second issue is that the effects of one type of spreading dynamics on another are typically asymmetric [21], requiring a modification of the symmetric assumption used in a recent work [19]. For example,

the spread of a disease can result in elevated crisis awareness and thus facilitate the spread of the information about the disease [17], but the spread of the information promotes more people to take preventive measures and consequently suppresses the epidemic spreading [26]. The third issue concerns the timing of the two types of spreading dynamics because they usually occur simultaneously on their respective layers and affect each other dynamically during the same time period [19].

Existing works treating the above three issues separately showed that each can have some significant effect on the epidemic and information spreading dynamics [16, 19, 40]. However, a unified framework encompassing the sophisticated consequences of all three issues is lacking. The purpose of this paper is to develop an asymmetrically interacting spreading-dynamics model to integrate the three issues so as to gain deep understanding into the intricate interplay between the epidemic and information spreading dynamics. When all three issues are taken into account simultaneously, we find that an epidemic outbreak on the contact layer can induce an outbreak on the communication layer, and information spreading can effectively raise the epidemic threshold, making the contact layer more resistant to disease spreading. When inter-layer correlation exists, the information threshold remains unchanged but the epidemic threshold can be enhanced, making the contact layer more resilient to epidemic outbreak. These results are established through analytic theory with extensive numerical support.

Results

In order to present our main results, we describe our two-layer network model and the dynamical process on each layer. We first treat the case where the double-layer networks are uncorrelated. We then incorporate layer-to-layer correlation in our analysis.

Model of communication-contact double-layer network. Communication-contact coupled layered networks are one class of multiplex networks [41]. In such a network, an individual (a node) not only connects with his/her friends on a physical contact layer (subnetwork), but also communicates with them through the (electronic) communication layer. The structures of the two layers can in general be quite different. For example, an indoor-type of individual has few friends in the real world but may have many friends in the cyber space, leading to a much higher degree in the communication layer than in the physical-contact layer. Generally, the degree-to-degree correlation between the two layers cannot be assumed to be strong.

Our correlated network model of communication-contact layers is constructed, as follows. Two subnetworks A and B with the same node set are first generated independently, where A and B denote the communication and contact layers, respectively. Each layer possesses a distinct internal structure, as characterized by measures such as the mean degree and degree distribution. Then each node of layer A is matched one-to-one with that of layer B according to certain rules.

In an uncorrelated double-layer network, the degree distribution of one layer is completely independent of the distributions of other layer. For example, a hub node with a large number of neighbors in one layer is not necessarily a hub node in the other layer. In contrast, in a correlated double-layer network, the degree distributions of the two layers are strongly dependent upon each other. In a perfectly correlated double-layer network, hub nodes in one layer must simultaneously be hub nodes in the other layer. Quantitatively, the Spearman rank correlation coefficient [39, 42] m_s , where $m_s \in [-1, 1]$ (see definition in **Methods**), can be used to characterize the degree correlation between the two layers. For $m_s > 0$, the greater the correlation coefficient, the larger degree a pair of counterpart nodes can have. For $m_s < 0$, as $|m_s|$ is decreased, a node of larger degree in one layer is matched with a node of smaller degree in the other layer.

Asymmetrically interacting spreading dynamics. The dynamical processes of disease and information spreading are typically asymmetrically coupled with each other. The dynamics component in our model can be described, as follows. In the communication layer (layer A), the classic susceptible-infected-recovered (SIR) epidemiological model [43] is used to describe the dissemination of information about the disease. In the SIR model, each node can be in one of the three states: (1) susceptible state (S) in which the individual has not received any information about the disease, (2) informed state (I), where the individual is aware of disease and is capable of transmitting the information to other individuals in the same layer, and (3) refractory state (R), in which the individual has received the information but is not willing to pass it on to other nodes. At each time step, the information can propagate from every informed node to all its neighboring nodes. If a neighbor is in the susceptible state, it will be informed with probability β_A . At the same time, each informed node can enter the recovering phase with probability μ_A . Once an informed node is recovered, it will remain in this state for all subsequent time. A node in layer A will get the information about the disease once its counterpart node in layer B is infected. As a result, dissemination of the information over layer A is facilitated by disease transmission on layer B .

The spreading dynamics in layer B can be described by the SIRV model [26], in which a fourth state, the state of vaccination (V), is introduced. Mathematically, the SIR component of the spreading dynamics is identical to the dynamics on layer A except for different infection and recovery rates, denoted by β_B and μ_B , respectively. If a node in layer B is in the susceptible state but its counterpart node in layer A is in the infected state, the node in layer B will be vaccinated with probability p . Disease transmission in the contact layer can thus be suppressed by dissemination of information in the communication layer. The two spreading processes and their dynamical interplay are illustrated schematically in Fig. 1. Without loss of generality, we set

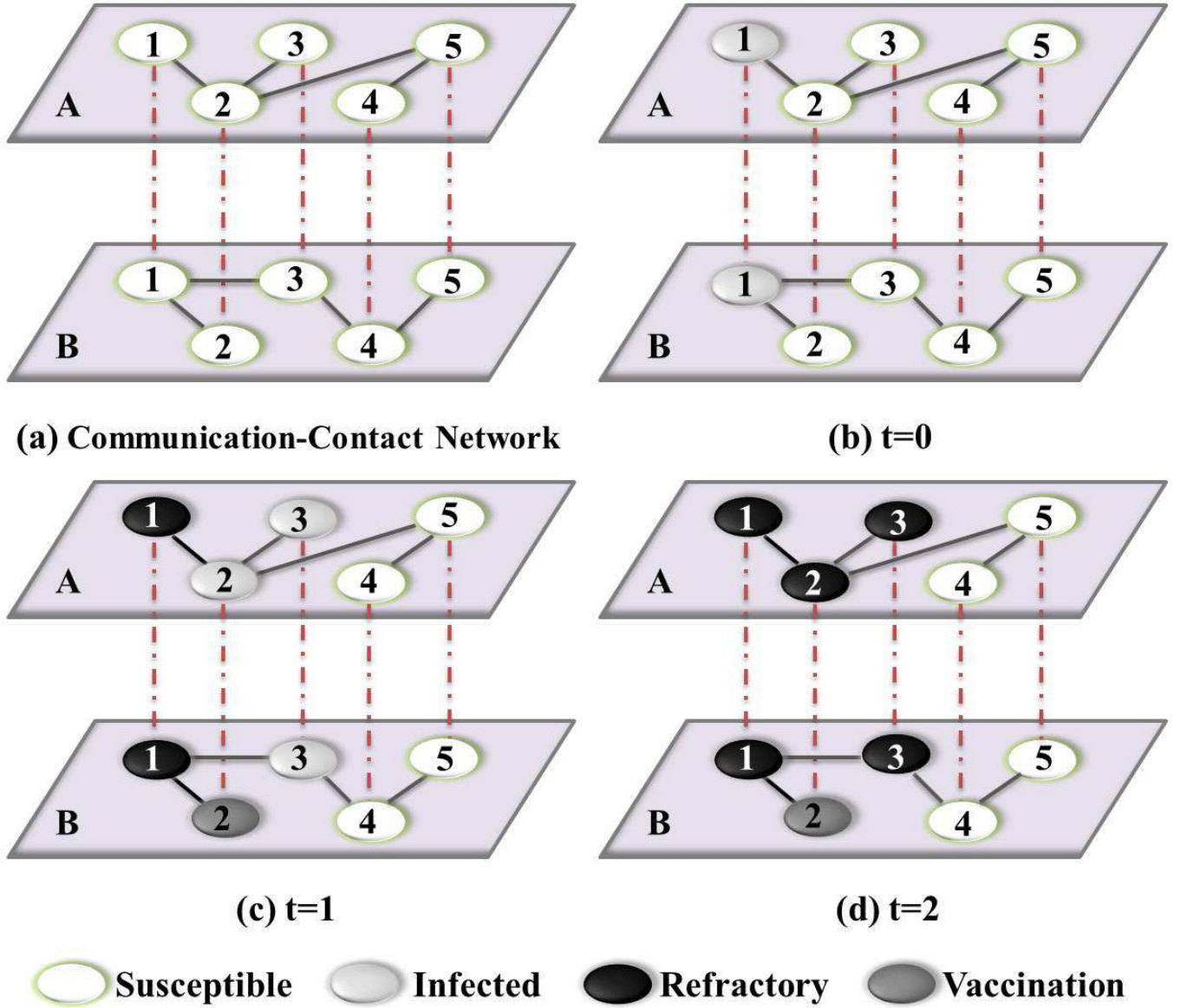


FIG. 1: Illustration of asymmetrically coupled spreading processes on a simulated communication-contact double-layer network. (a) Communication and contact networks, denoted as layer A and layer B , respectively, each of five nodes. (b) At $t = 0$, node B_1 in layer B is randomly selected as the initial infected node and its counterpart, node A_1 in layer A , gains the information that B_1 is infected, while all other pairs of nodes, one from layer A and another from layer B , are in the susceptible state. (c) At $t = 1$, within layer A the information is transmitted from A_1 to A_2 with probability β_A . Node B_3 in layer B can be infected by node B_1 with probability β_B and, if it is indeed infected, its corresponding node A_3 in layer A gets the information as well. Since, by this time, A_2 is already aware of the infection spreading, its counterpart B_2 in layer B is vaccinated, say with probability p . At the same time, node A_1 in layer A and its counterpart B_1 in layer B enter into the refractory state with probability μ_A and μ_B , respectively. (d) At $t = 2$, all infected (or informed) nodes in both layers can no longer infect others, and start recovering from the infection. In both layers, the spreading dynamics terminate by this time.

$$\mu_A = \mu_B = 1.$$

Theory of spreading dynamics in uncorrelated double-layer networks. Two key quantities in the dynamics of spreading are the outbreak threshold and the fraction of infected nodes in the final steady state. We develop a theory to predict these quantities for both information and epidemic spreading in the double-layer network. In particular, we adopt the heterogeneous mean-field theory [44] to uncorrelated double-layer networks.

Let $P_A(k_A)$ and $P_B(k_B)$ be the degree distributions of layers A and B , with mean degree $\langle k_A \rangle$ and $\langle k_B \rangle$, respectively. We assume that the subnetworks associated with both layers are random with no degree correlation. The time evolution of the

epidemic spreading is described by the variables $s_{k_A}^A(t)$, $\rho_{k_A}^A(t)$, and $r_{k_A}^A(t)$, which are the densities of the susceptible, informed, and recovered nodes of degree k_A in layer A at time t , respectively. Similarly, $s_{k_B}^B(t)$, $\rho_{k_B}^B(t)$, $r_{k_B}^B(t)$, and $v_{k_B}^B(t)$ respectively denote the susceptible, infected, recovered, and vaccinated densities of nodes of degree k_B in layer B at time t .

The mean-field rate equations of the information spreading in layer A are

$$\frac{ds_{k_A}^A(t)}{dt} = -s_{k_A}^A(t)[\beta_A k_A \Theta_A(t) + \beta_B \Theta_B(t) \sum_{k_B} k_B P_B(k_B)], \quad (1)$$

$$\frac{d\rho_{k_A}^A(t)}{dt} = s_{k_A}^A(t)[\beta_A k_A \Theta_A(t) + \beta_B \Theta_B(t) \sum_{k_B} k_B P_B(k_B)] - \rho_{k_A}^A(t), \quad (2)$$

$$\frac{dr_{k_A}^A(t)}{dt} = \rho_{k_A}^A(t). \quad (3)$$

The mean-field rate equations of epidemic spreading in layer B are given by

$$\frac{ds_{k_B}^B(t)}{dt} = -s_{k_B}^B(t)\beta_B k_B \Theta_B(t) - p\beta_A \Theta_A(t) \sum_{k_A} s_{k_A}^A(t)k_A P_A(k_A), \quad (4)$$

$$\frac{d\rho_{k_B}^B(t)}{dt} = s_{k_B}^B(t)\beta_B k_B \Theta_B(t) - \rho_{k_B}^B(t), \quad (5)$$

$$\frac{dr_{k_B}^B(t)}{dt} = \rho_{k_B}^B(t), \quad (6)$$

$$\frac{dv_{k_B}^B(t)}{dt} = p\beta_A \Theta_A(t) \sum_{k_A} s_{k_A}^A(t)k_A P_A(k_A), \quad (7)$$

where $\Theta_A(t)$ ($\Theta_B(t)$) is the probability that a neighboring node in layer A (layer B) is in the informed (infected) state (See **Methods** for details).

From Eqs. (1)-(7), the density associated with each distinct state in layer A or B is given by

$$X_h(t) = \sum_{k_h=1}^{k_{h,max}} P_h(k_h) X_{k_h}^h(t), \quad (8)$$

where $h \in \{A, B\}$, $X \in \{S, I, R, V\}$, and $k_{h,max}$ denotes the largest degree of layer h . The final densities of the whole system can be obtained by taking the limit $t \rightarrow \infty$.

Due to the complicated interaction between the disease and information spreading processes, it is not feasible to derive the exact threshold values. We resort to a linear approximation method to get the outbreak threshold of information spreading in layer A (see Supporting Information for details) as

$$\beta_{Ac} = \begin{cases} \beta_{Au}, & \text{for } \beta_B \leq \beta_{Bu} \\ 0, & \text{for } \beta_B > \beta_{Bu}, \end{cases} \quad (9)$$

where

$$\begin{aligned} \beta_{Au} &\equiv \langle k_A \rangle / (\langle k_A^2 \rangle - \langle k_A \rangle) \text{ and} \\ \beta_{Bu} &\equiv \langle k_B \rangle / (\langle k_B^2 \rangle - \langle k_B \rangle) \end{aligned}$$

denote the outbreak threshold of information spreading in layer A when it is isolated from layer B , and that of epidemic spreading in layer B when the coupling between the two layers is absent, respectively.

Equation (9) has embedded within it two distinct physical mechanisms for information outbreak. The first is the intrinsic information spreading process on the isolated layer A without the impact of the spreading dynamics from layer B . For $\beta_B > \beta_{Bu}$, the outbreak of epidemic will make a large number of nodes in layer A “infected” with the information, even if on layer A , the information itself cannot spread through the population efficiently. In this case, the information outbreak has little effect on the epidemic spreading in layer B because very few nodes in this layer are vaccinated. We thus have $\beta_{Bc} \approx \beta_{Bu}$ for $\beta_A \leq \beta_{Au}$.

However, for $\beta_A > \beta_{Au}$, epidemic spreading in layer B is restrained by information spread, as the informed nodes in layer A tend to make their counterpart nodes in layer B vaccinated. Once a node is in the vaccination state, it will no longer be infected. In a general sense, vaccination can be regarded as a type of “disease,” as every node in layer B can be in one of the two states:

infected or vaccinated. Epidemic spreading and vaccination can thus be viewed as a pair of competing “diseases” spreading in layer B [20]. As pointed out by Karrer and Newman [20], in the limit of large network size N , the two competing diseases can be treated as if they were in fact spreading non-concurrently, one after the other.

Initially, both epidemic and vaccination spreading processes exhibit exponential growth (see Supporting Information). We can thus obtain the ratio of their growth rates as

$$\theta = \frac{\beta_B \beta_{Au}}{\beta_A \beta_{Bu}}. \quad (10)$$

For $\theta > 1$, the epidemic disease spreads faster than the vaccination. In this case, the vaccination spread is insignificant and can be neglected. For $\theta < 1$, information spreads much faster than the disease, in accordance with the situation in a modern society. Given that the vaccination and epidemic processes can be treated successively and separately, the epidemic outbreak threshold can be derived by a bond percolation analysis [20, 45] (see details in Supporting Information). We obtain

$$\beta_{Bc} = \frac{\langle k_B \rangle}{(1 - p S_A)(\langle k_B^2 \rangle - \langle k_B \rangle)}, \quad (11)$$

where S_A is the density of the informed population, which can be obtained by solving Eqs. (S18) and (S19) in Supporting Information. For $\theta < 1$, we see from Eq. (11) that the threshold for epidemic outbreak can be enhanced by the following factors: strong heterogeneity in the communication layer, large information-transmission rate, and large vaccination rate.

Simulation results for uncorrelated networks. We use the standard configuration model to generate networks with power-law degree distributions [46–48] for the communication subnetwork (layer A). The contact subnetwork in layer B is of the Erdős and Rényi (ER) type [49]. We use the notation SF-ER to denote the double-layer network. The sizes of both layers are set to be $N_A = N_B = 2 \times 10^4$ and their average degrees are $\langle k_A \rangle = \langle k_B \rangle = 8$. The degree distribution of the communication layer is $P_A(k_A) = \zeta k_A^{-\gamma_A}$ with the coefficient $\zeta = 1 / \sum_{k_{min}}^{k_{max}} k_A^{-\gamma_A}$ and the maximum degree $k_{max} \sim N^{1/(\gamma_A-1)}$. We focus on the case of $\gamma_A = 3.0$ here in the main text (the results for other values of the exponent, e.g., $\gamma_A = 2.7$ and 3.5 , are similar, which are presented in Supporting Information). The degree distribution of the contact layer is $P_B(k_B) = e^{-\langle k_B \rangle} \langle k_B \rangle^{k_B} / k_B!$. To initiate an epidemic spreading process, a node in layer B is randomly infected and its counterpart node in layer A is thus in the informed state, too. We implement the updating process with parallel dynamics, which is widely used in statistical physics [50] (see Sec. S3A in Supporting Information for more details). The spreading dynamics terminates when all infected nodes in both layers are recovered, and the final densities R_A , R_B , and V_B are then recorded.

For epidemiological models [e.g., the susceptible-infected-susceptible (SIS) and SIR] on networks with a power-law degree distribution, the finite-size scaling method may not be effective to determine the critical point of epidemic dynamics [51, 52], because the outbreak threshold depends on network size and it goes to zero in the thermodynamic limit [43, 53]. Therefore, we employ the *susceptibility measure* [52] χ to numerically determine the size-dependent outbreak threshold:

$$\chi = N \frac{\langle r^2 \rangle - \langle r \rangle^2}{\langle r \rangle}, \quad (12)$$

where N is network size ($N = N_A = N_B$), and r denotes the final outbreak ratio such as the final densities R_A and R_B of the recovered nodes in layers A and B , respectively. We use 2×10^3 independent dynamic realizations on a fixed double-layer network to calculate the average value of χ for the communication layer for each value of β_A . As shown in Fig. 2(a), χ exhibits a maximum value at β_{Ac} , which is the threshold value of the information spreading process. The simulations are further implemented using 30 different two-layer network realizations to obtain the average value of β_{Ac} . The identical simulation setting is used for all subsequent numerical results, unless otherwise specified. Figure 2(b) shows the information threshold β_{Ac} as a function of the disease-transmission rate β_B . Note that the statistical errors are not visible here (same for similar figures in the paper), as they are typically vanishingly small. We see that the behavior of the information threshold can be classified into two classes, as predicted by Eq. (9). In particular, for $\beta_B \leq \beta_{Bu} = 1/\langle k_B \rangle = 0.125$, the disease transmission on layer B has little impact on the information threshold on layer A , as we have $\beta_{Ac} \approx \beta_{Au} = \langle k_A \rangle / (\langle k_A^2 \rangle - \langle k_A \rangle) \approx 0.06$. For $\beta_B > \beta_{Bu}$, the outbreak of epidemic on layer B leads to $\beta_{Ac} = 0.0$. Comparison of the information thresholds for different vaccination rates shows that the value of the vaccination probability p has essentially no effect on β_{Ac} .

Figure 3 shows the effect of the information-transmission rate β_A and the vaccination rate p on the epidemic threshold β_{Bc} . From Fig. 3(a), we see that the value of β_{Bc} is not influenced by β_A for $\beta_A \leq \beta_{Au} \approx 0.06$, whereas β_{Bc} increases with β_A . For $p = 0.5$, the analytical results from Eq. (11) are consistent with the simulated results. However, deviations occur for larger values of p , e.g., $p = 0.9$, because the effect of information spreading is over-emphasized in cases where the two types of spreading dynamics are treated successively but not simultaneously. The gap between the theoretical and simulated thresholds diminishes as the network size is increased, validating applicability of the analysis method that, strictly speaking, holds only in the thermodynamic limit [20] (see details in Supporting Information). Note that a giant residual cluster does not exist in layer B

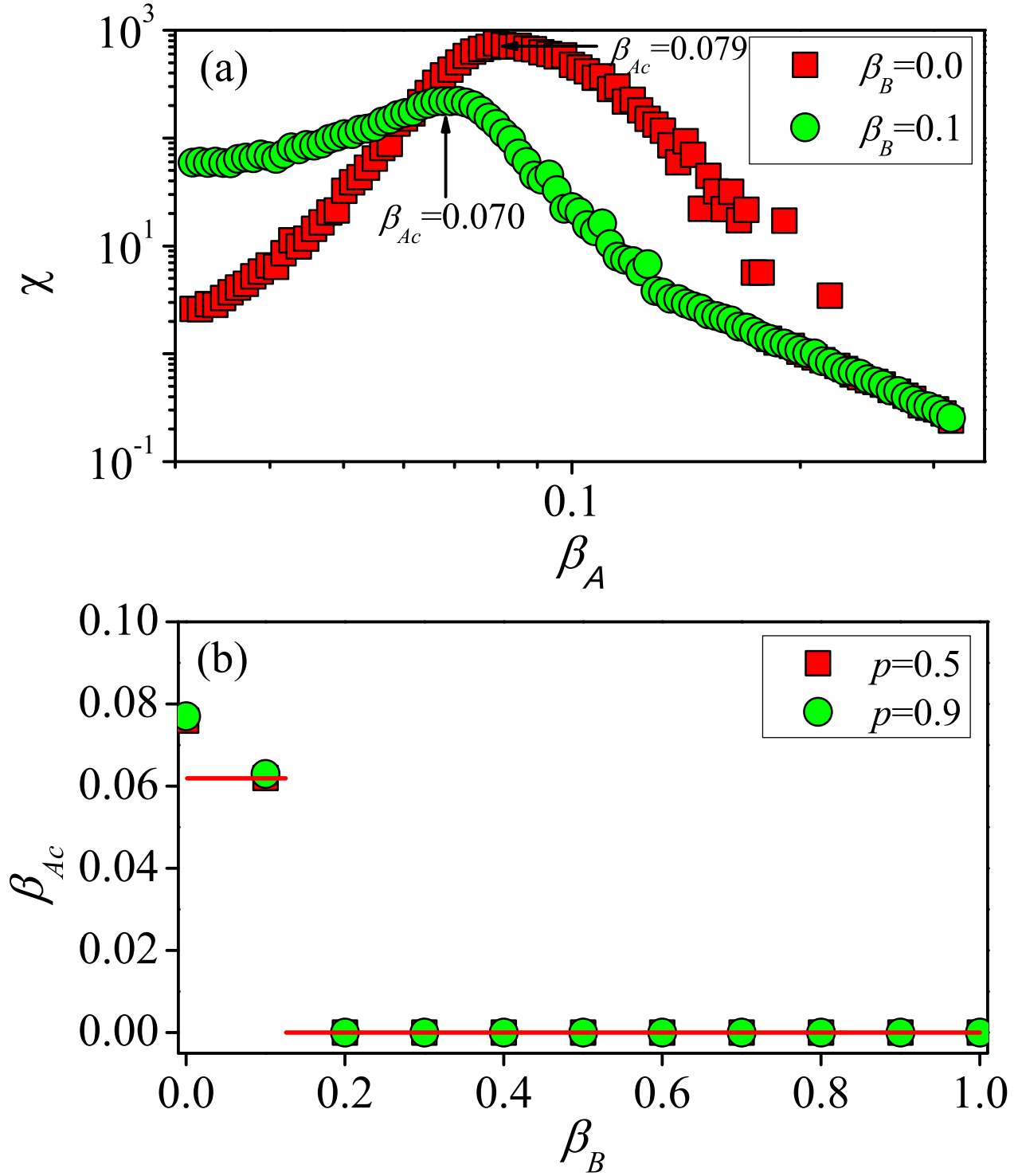


FIG. 2: On SF-ER networks, (a) susceptibility measure χ as a function of the information-transmission rate β_A for $p = 0.5$, $\beta_B = 0.0$ (red squares) and $\beta_B = 0.1$ (green circles), (b) threshold β_{Ac} of information spreading as a function of the disease-transmission rate β_B for vaccination rate $p = 0.5$ (red squares) and $p = 0.9$ (green circles), where the red solid lines are analytical predictions from Eq. (9).

for $p = 0.9$ and $\beta_A \geq 0.49$, ruling out epidemic outbreak. The phase diagram indicating the possible existence of a giant residual cluster [Eq. (S20) in Supporting Information] is shown in the inset of Fig. 3(a), where in phase II, there is no such cluster. In Fig. 3(b), a large value of p causes β_{Bc} to increase for $\beta_A > \beta_{Au}$. We observe that, similar to Fig. 3(a), for relatively large values of p , say $p \geq 0.8$, the analytical prediction deviates from the numerical results. The effects of network size N , exponent γ_A and SF-SF network structure on the information and epidemic thresholds are discussed in detail in Supporting Information.

The final dynamical state of the double-layer spreading system is shown in Fig. 4. From Fig. 4(a), we see that the final recovered density R_A for information increases with β_A and β_B rapidly for $\beta_A \leq \beta_{Au}$ and $\beta_B \leq \beta_{Bu}$. Figure 4(b) reveals that the recovered density R_B for disease decreases with β_A . We see that a large value of β_A can prevent the outbreak of epidemic for small values of β_B , as $R_B \rightarrow 0$ for $\beta_B = 0.2$ and $\beta_A \geq 0.5$ (the red solid line). From Fig. 4(c), we see that, with the increase in β_A , more nodes in layer B are vaccinated. It is interesting to note that the vaccinated density V_B exhibits a maximum value if β_A is not large. Figure 4 shows that the maximum value of V_B is about 0.32, which occurs at $\beta_B \approx 0.20$, for $\beta_A = 0.2$. Combining with Fig. 3(a), we find that the corresponding point of the maximum value $\beta_B \approx 0.20$ is close to $\beta_{Bc} \approx 0.16$ for $p = 0.5$. This is because the transmission of disease has the opposite effects on the vaccinations. For $\beta_B \leq \beta_{Bc}$, the newly infected nodes in layer B will facilitate information spreading in layer A , resulting in more vaccinated nodes. For $\beta_B > \beta_{Bc}$, the epidemic spreading will make a large number of nodes infected, reducing the number of nodes that are potentially to be vaccinated. For relatively large values of β_A , information tends to spread much faster than the disease for $\beta_B \leq \beta_{Bc}$, e.g., $\theta \approx 0.21$ for $\beta_A = 0.5$, $p = 0.5$, $\beta_{Bc} \approx 0.22$, and $\theta \approx 0.12$ for $\beta_A = 0.9$, $p = 0.5$, and $\beta_{Bc} \approx 0.23$. In this case, the effect of disease transmission on information spreading is negligible. The densities of the final dynamical states for SF-SF networks are also shown in Supporting Information, and we observe similar behaviors.

Spreading dynamics on correlated double-layer networks. In realistic multiplex networks certain degree of inter-layer correlations is expected to exist [35]. For example, in social networks, positive inter-layer correlation is more common than negative correlation [54, 55]. That is, an “important” individual with a large number of links in one network layer (e.g., representing one type of social relations) tends to have many links in other types of network layers that reflect different kinds of social relations. Recent works have shown that inter-layer correlation can have a large impact on the percolation properties of multiplex networks [37, 39]. Here, we investigate how the correlation between the communication and contact layers affects the information and disease spreading dynamics. To be concrete, we focus on the effects of positive correlation on the two types of spreading dynamics. It is necessary to construct a two-layer correlated network with adjustable degree of inter-layer correlation. This can be accomplished by first generating a two-layer network with the maximal positive correlation, where each layer has the same structure as uncorrelated networks. Then, Nq pairs of counterpart nodes, in which q is the rematching probability, are rematched randomly, leading to a two-layer network with weaker inter-layer correlation. The inter-layer correlation after rematching is given by (see **Methods**)

$$m_s \approx 1 - q, \quad (13)$$

which is consistent with the numerical results [e.g., see inset of Fig. 5(a) below]. For SF-ER networks with fixed correlation coefficient, the mean-field rate equations of the double-layer system cannot be written down because the concrete expressions of the conditional probabilities $P(k_B|k_A)$ and $P(k_A|k_B)$ are no longer available.

We investigate how the rematching probability q affects the outbreak thresholds in both the communication and epidemic layers. As shown in Fig. 5, we compare the case of $q = 0.8$ with that of $q = 0.0$. From Fig. 5(a), we see that q has little impact on the outbreak threshold β_{Ac} of the communication layer [with further support in Fig. 6(a), and analytic explanation using ER-ER correlated layered networks in Supporting Information]. We also see that the value of β_{Ac} for ER-ER layered networks with the same mean degree is greater because of the homogeneity in the degree distribution of layer A . Figures 5(b) and 6(b) show that β_{Bc} decreases with q or, equivalently, β_{Bc} increases with m_s . This is because stronger inter-layer correlation can increase the probability for nodes with large degrees in layer B to be vaccinated, thus effectively preventing the outbreak of epidemic [see also Eqs. (S38)-(S41) in Supporting Information]. Figure 7 shows the final densities of different populations, providing the consistent result that, with the increase (decrease) of q (m_s), the final densities R_A and R_B increase but the density V_B decreases. For SF-SF networks, we obtain similar results (shown in Supporting Information).

Discussion

To summarize, we have proposed an asymmetrically interacting, double-layer network model to elucidate the interplay between information diffusion and epidemic spreading, where the former occurs on one layer (the communication layer) and the latter on the counterpart layer. A mean-field based analysis and extensive computations reveal an intricate interdependence of two basic quantities characterizing the spreading dynamics on both layers: the outbreak thresholds and the final fractions of infected nodes. In particular, on the communication layer, the outbreak of the information about the disease can be triggered not

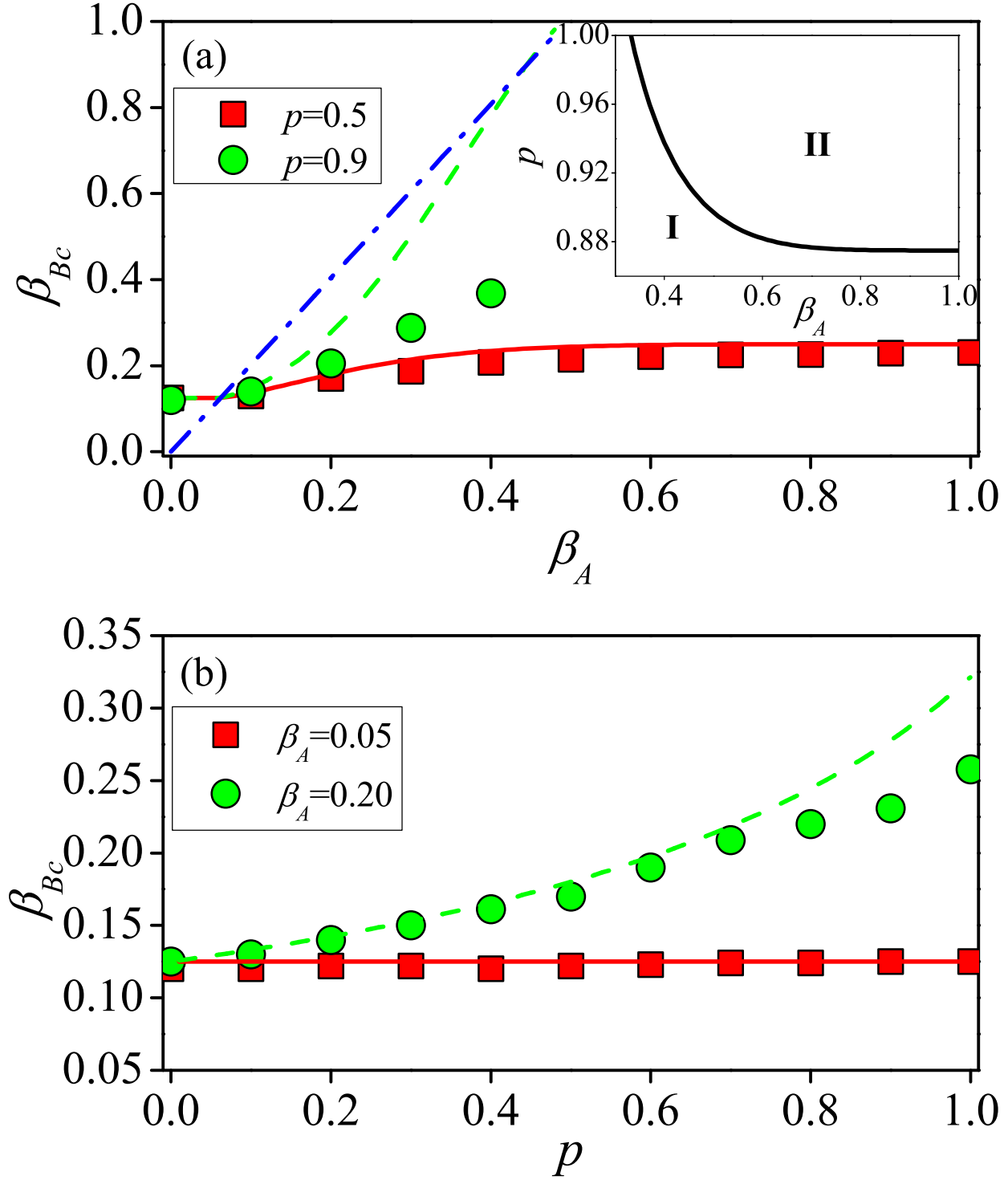


FIG. 3: For SF-ER double-layer networks, epidemic threshold β_{Bc} as a function of the information-transmission rate β_A (a) and the vaccination rate p (b). In (a), the red solid ($p = 0.5$) and green dashed ($p = 0.9$) lines are the analytical predictions from Eq. (11), and the blue dot-dashed line denotes the case of $\theta = 1$ from Eq. (10). Inset of (a) shows the condition under which a giant residual cluster of layer B exists [from Eq. (S20) in Supporting Information] in phase I. In (b), the red solid line ($\beta_A = 0.05$) corresponds to $\beta_{Bc} = \beta_{Bu}$, and the green dashed line ($\beta_A = 0.20$) is the analytical prediction from Eq. (11).

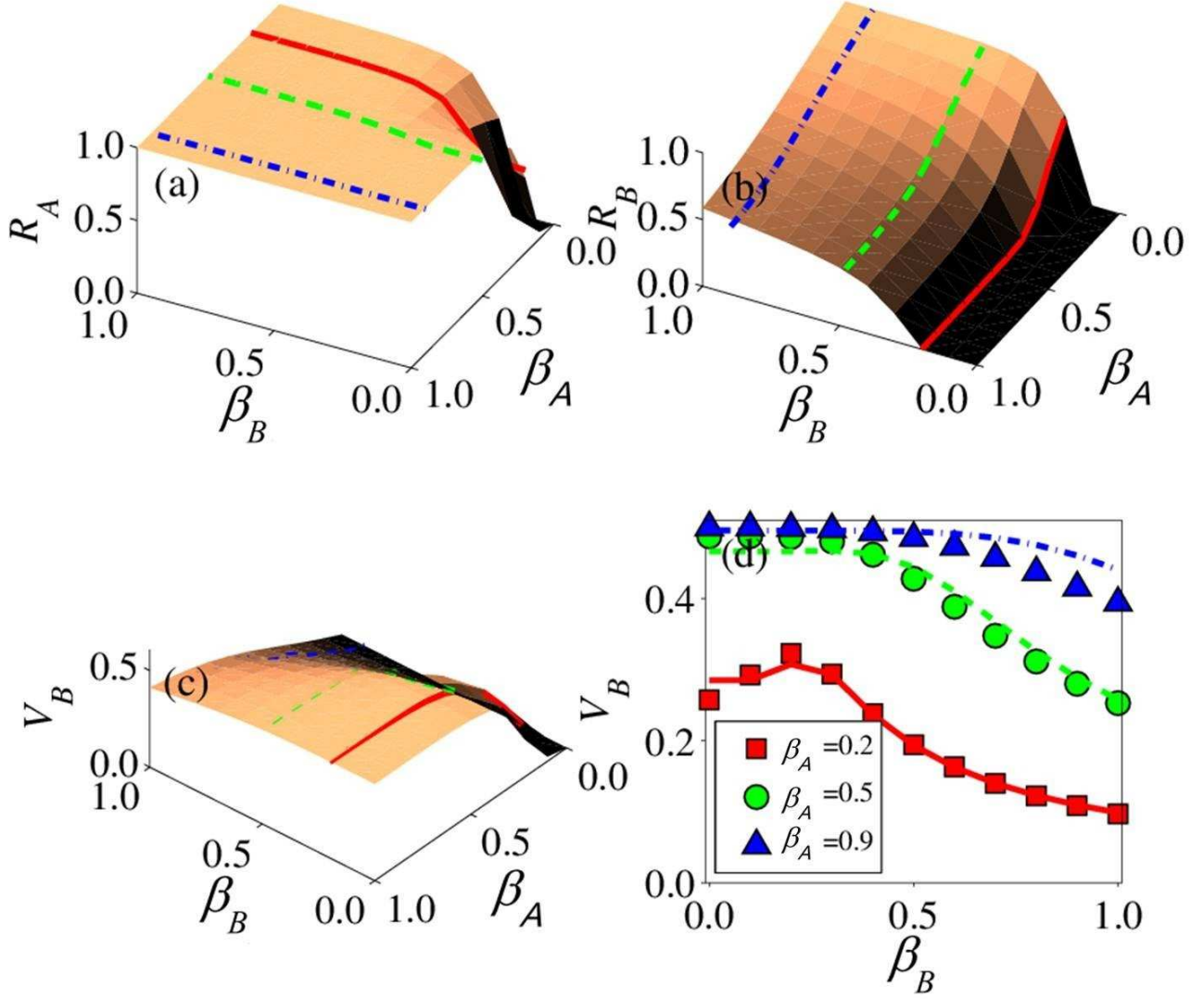


FIG. 4: For SF-ER networks, final density in each state versus the parameters β_A and β_B : (a) recovered density R_A , (b) recovered density R_B , (c) the vaccination density V_B , and (d) V_B versus β_B for $\beta_A = 0.2, 0.5, 0.9$. The value of parameter p is 0.5. Different lines are the numerical solutions of Eqs. (1)-(8) in the limit $t \rightarrow \infty$. In (a) and (d), we select three different values of β_A (0.2, 0.5, and 0.9), corresponding to the red solid, green dashed, and blue dot-dashed lines, respectively. In (b) and (c), three different values of β_B are chosen (0.2, 0.5, and 0.9), corresponding to the red solid, green dashed, and blue dot-dashed lines, respectively.

only by its own spreading dynamics but also by the epidemic outbreak on the counter-layer. In addition, high disease and information-transmission rates can enhance markedly the final density of the informed or refractory population. On the layer of physical contact, the epidemic threshold can be increased but only if information itself spreads through the communication layer at a high rate. The information spreading can greatly reduce the final refractory density for the disease through vaccination. While a rapid spread of information will prompt more nodes in the contact layer to consider immunization, the authenticity of the information source must be verified before administrating large-scale vaccination.

We have also studied the effect of inter-layer correlation on the spreading dynamics, with the finding that stronger correlation has no apparent effect on the information threshold, but it can suppress the epidemic spreading through timely immunization of large-degree nodes [56]. These results indicate that it is possible to effectively mitigate epidemic spreading through information diffusion, e.g., by informing the high-centrality hubs about the disease.

The challenges of studying the intricate interplay between social and biological contagions in human populations are generat-

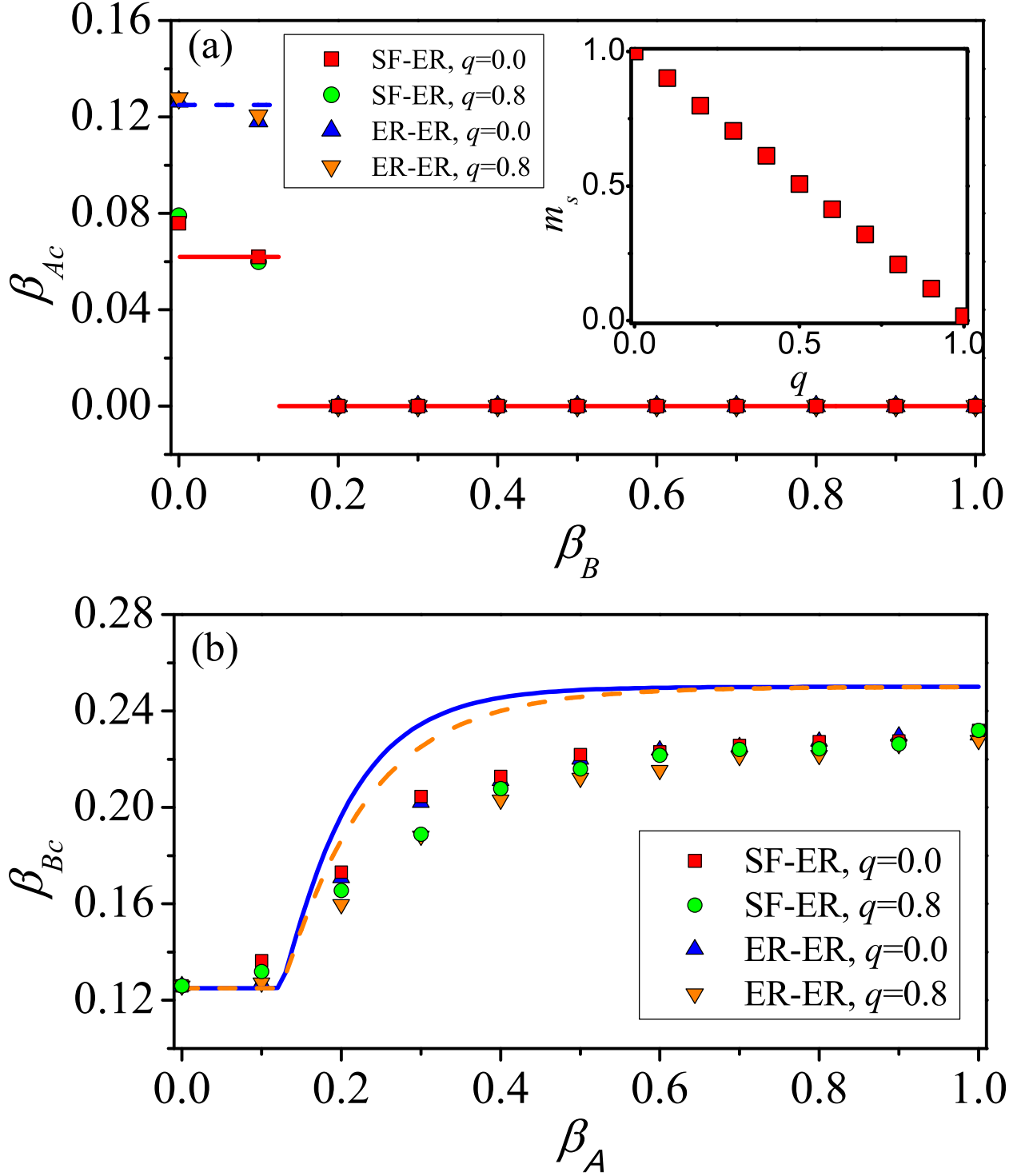


FIG. 5: For two-layer correlated networks with vaccination probability $p = 0.5$, the effect of one type of spreading dynamics on the outbreak threshold of the counter-type spreading dynamics. (a) β_{Ac} versus β_B on SF-ER networks with $q = 0.0$ (red squares) and $q = 0.8$ (green circles), and ER-ER networks with $q = 0.0$ (blue up triangles) and $q = 0.8$ (orange down triangles). Red solid (SF-ER) and blue dashed (ER-ER) lines are the analytical predictions from Eq. (9) and Eq. (S37) (in Supporting Information), respectively. The inset shows the inter-layer correlation m_s as a function of rematching probability q . (b) β_{Bc} versus β_A on SF-ER networks with $q = 0.0$ (red squares) and $q = 0.8$ (green circles), and ER-ER networks with $q = 0.0$ (blue up triangles) and $q = 0.8$ (orange down triangles). Blue solid ($q = 0.0$) and orange dashed ($q = 0.8$) lines are the analytical predictions for ER-ER networks from Eqs. (S38)-(S41) in Supporting Information.

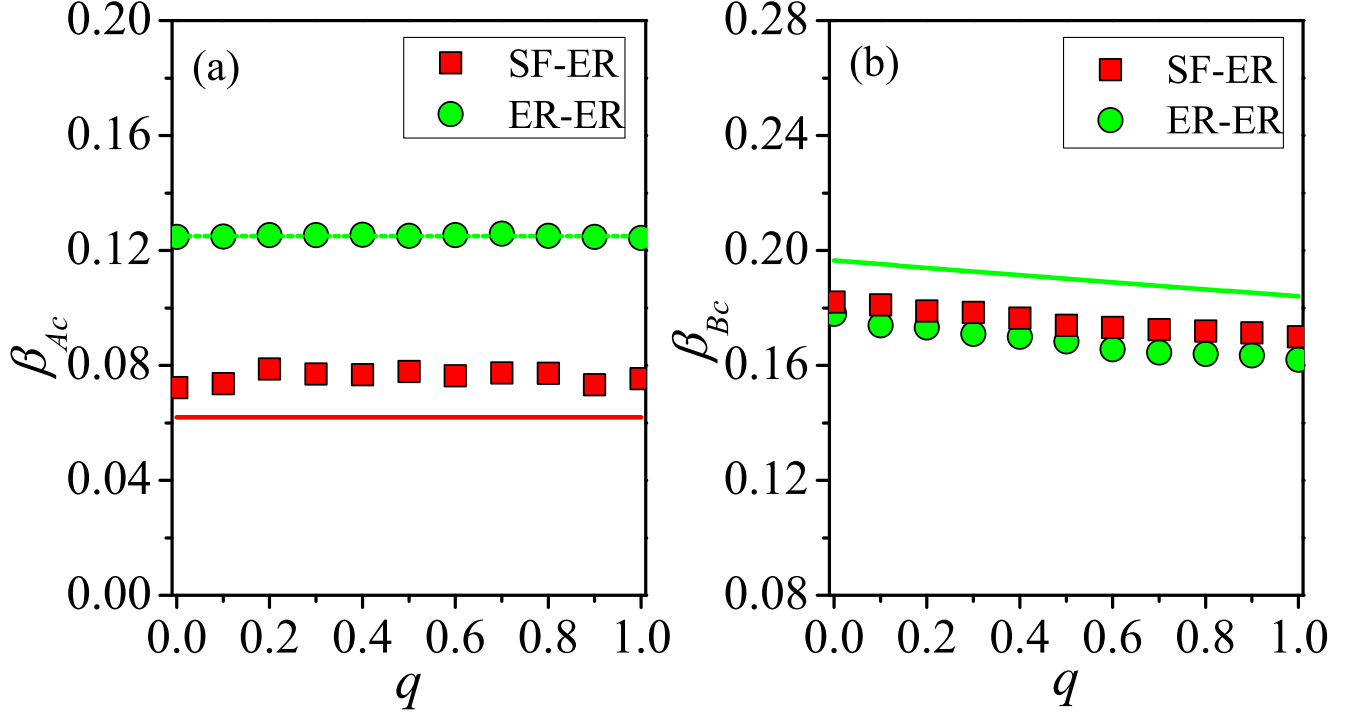


FIG. 6: Effect of varying the rematching probability on outbreak thresholds of the two types of spreading dynamics. (a) β_{Ac} versus q on SF-ER (red squares) and ER-ER networks (green circles) for $\beta_B = 0.05$ and $p = 0.5$. Red Solid (SF-ER) and green dashed (ER-ER) lines are analytical predictions from Eq. (9) and Eq. (S37) in Supporting Information, respectively. (b) β_{Bc} versus q on SF-ER (red squares) and ER-ER networks (green circles) for $\beta_A = 0.2$ and $p = 0.5$. Green solid line is analytical prediction for ER-ER networks from Eqs. (S38)-(S41) in Supporting Information.

ing interesting science [57]. In this work, we study asymmetrically interacting information-disease dynamics theoretically and computationally, with implications to behavior-disease coupled systems and articulation of potential epidemic-control strategies. Our results would stimulate further works in the more realistic situation of asymmetric interactions.

During the final writing of this paper, we noted one preprint posted online studying the dynamical interplay between awareness and epidemic spreading in multiplex networks [58]. In that work, the two competing infectious strains are described by two SIS processes. The authors find that the epidemic threshold depends on the topological structure of the multiplex network and the interrelation with the awareness process by using a Markov-chain approach. Our work thus provides further understanding and insights into spreading dynamics on multi-layer coupled networks.

Methods

Mean-Field theory for the uncorrelated double-layer networks. To derive the mean-field rate equations for the density variables, we consider the probabilities that node A_i in layer A and node B_i in layer B become infected during the small time interval $[t, t + dt]$. On the communication layer, a susceptible node A_i of degree k_A can obtain the information in two ways: from its neighbors in the same layer and from its counterpart node in layer B . For the first route, the probability that node A_i receives information from one of its neighbors is $k_A \beta_A \Theta_A(t) dt$, where $\Theta_A(t)$ is the probability that a neighboring node is in the informed state [59] and is given by

$$\Theta_A(t) = \frac{\sum_{k'_A} (k'_A - 1) P_A(k'_A) \rho_{k'_A}^A(t)}{\langle k_A \rangle}, \quad (14)$$

where $\langle k_A \rangle = \sum_{k_A} k_A P_A(k_A)$. To model the second scenario, we note that, due to the asymmetric coupling between the two layers, a node in layer A being susceptible requires that its counterpart node in layer B be susceptible, too. A node in

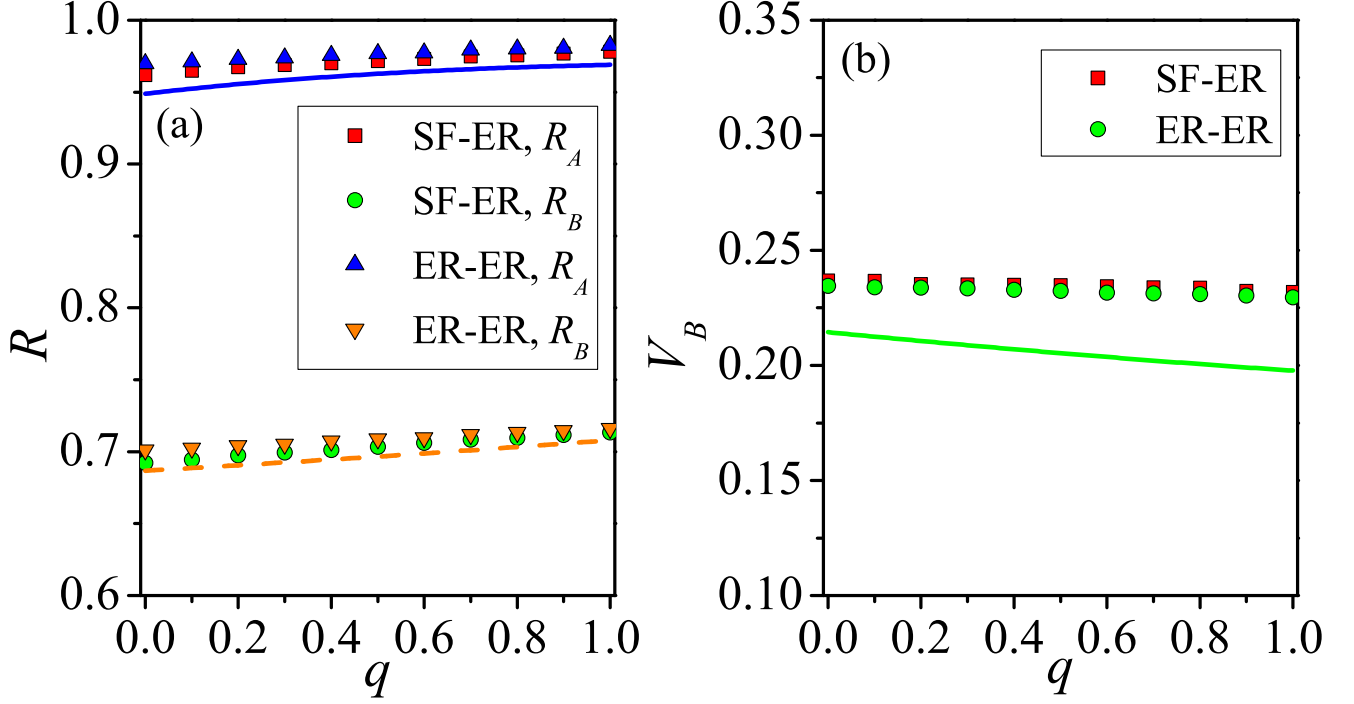


FIG. 7: Effect of rematching probability on the final state. (a) R_A versus q on SF-ER (red squares) and ER-ER networks (blue up triangles), R_B versus q on SF-ER (green circles) and ER-ER networks (orange down triangles). (b) V_B versus q on SF-ER (red squares) and ER-ER networks (green circles). Different lines represent the analytic solutions for ER-ER networks, calculated by summing the final densities of all degrees from Eqs. (S28)-(S34) in Supporting Information. The parameter setting is $\beta_A = 0.2$, $\beta_B = 0.4$ and $p = 0.5$.

the communication layer will get the information about the disease once its counterpart node in layer B is infected, which occurs with the probability $\sum_{k_B} P(k_B|k_A) k_B \beta_B \Theta_B(t) dt$, where $P(k_B|k_A)$ denotes the conditional probability that a node of degree k_A in layer A is linked to a node of degree k_B in layer B , and $k_B \beta_B \Theta_B(t) dt$ is the probability for a counterpart node of degree k_B to become infected in the time interval $[t, t + dt]$. If the subnetworks in both layers are not correlated, we have $P(k_B|k_A) = P_B(k_B)$. The mean-field rate equations of the information spreading in layer A are Eqs. (1)-(3).

On layer B , a susceptible node B_i of degree k_B may become infected or vaccinated in the time interval $[t, t + dt]$. This can occur in two ways. Firstly, it may be infected by a neighboring node in the same layer with the probability $k_B \beta_B \Theta_B(t) dt$, where $\Theta_B(t)$ is the probability that a neighbor is in the infected state and is given by

$$\Theta_B(t) = \frac{\sum_{k'_B} (k'_B - 1) P_B(k'_B) \rho_{k'_B}^B(t)}{\langle k_B \rangle}, \quad (15)$$

where $\langle k_B \rangle = \sum_{k_B} k_B P_B(k_B)$. Secondly, if its counterpart node in layer A has already received the information from one of its neighbors, it will be vaccinated with probability p . The probability for a node in layer B to be vaccinated, taking into account the interaction between the two layers, is $p \sum_{k_A} P(k_A|k_B) s_{k_A}^A(t) \beta_A k_A \Theta_A(t) dt$, where $P(k_A|k_B)$ denotes the conditional probability that a node of degree k_B in layer B is linked to a node of degree k_A in layer A , and $s_{k_A}^A(t) \beta_A k_A \Theta_A(t) dt$ is the informed probability for the counterpart node of degree k_A in the susceptible state [$P(k_A|k_B) = P_A(k_A)$ for $m_s = 0$]. The mean-field rate equations of epidemic spreading in layer B are Eqs. (4)-(7). We note that the second term on the right side of Eq. (4) does not contain the variable $s_{k_B}^B(t)$ because a node in layer B must be in the susceptible state if its counterpart node in layer A is in the susceptible state.

Spearman rank correlation coefficient. The correlation between the layers can be quantified by the Spearman rank correlation coefficient [39, 42] defined as

$$m_s = 1 - 6 \frac{\sum_{i=1}^N \Delta_i^2}{N(N^2 - 1)}, \quad (16)$$

where N is network size and Δ_i denotes the difference between node i 's degrees in the two layers. When a node in layer A is matched with a random node in layer B , m_s is approximately zero in the thermodynamic limit. In this case, the double-layer network is uncorrelated [39, 42]. When every node has the same rank of degree in both layers, we have $m_s \approx 1$. In this case, there is a maximally positive inter-layer correlation where, for example, the hub node with the highest degree in layer A is matched with the largest hub in layer B , and the same holds for the nodes with the smallest degree. In the case of maximally negative correlation, the largest hub in one layer is matched with a node having the minimal degree in the other layer, so we have $m_s \approx -1$.

In a double-layer network with the maximally positive correlation, any pair of nodes having the same rank of degree in the respective layers are matched, i.e., $\Delta_i = 0$ for any pair of nodes A_i and B_i . We thus have $m_s = 1$, according to Eq. (16). After random rematching, a pair of nodes have $\Delta_i = 0$ with probability $1 - q$ and a random difference Δ'_i with probability q . Equation (16) can then be rewritten as

$$m_s = 1 - 6 \frac{q \sum_{i=1}^N \Delta_i'^2}{N(N^2 - 1)}. \quad (17)$$

When all nodes are randomly rematched, the layers in the network are completely uncorrelated, i.e., $m_s \approx 0$. In this case, we have

$$6 \frac{\sum_{i=1}^N \Delta_i'^2}{N(N^2 - 1)} \approx 1. \quad (18)$$

Submitting Eq. (18) into Eq. (17), the inter-layer correlation after rematching is given by

$$m_s \approx 1 - q. \quad (19)$$

* Electronic address: tangminghuang521@hotmail.com

- [1] Pastor-Satorras, R. & Vespignani, A. Epidemic Spreading in Scale-Free Networks. *Phys. Rev. Lett.* **86**, 3200 (2001).
- [2] Tang, M., Liu, Z., & Li, B. Epidemic spreading by objective traveling. *Europhys. Lett.* **87**, 18005 (2009).
- [3] Shu, P., Tang, M., Gong, K., & Liu, Y. Effects of weak ties on epidemic predictability on community networks. *Chaos* **22**, 043124 (2012).
- [4] Wang, L., Wang, Z., Zhang, Y., & Li, X. How human location-specific contact patterns impact spatial transmission between populations? *Sci. Rep.* **3**, 1468 (2013).
- [5] Gross, T., Dommar D'Lima, C. & Blasius, B. Epidemic dynamics on an adaptive network. *Phys. Rev. Lett.* **96**, 208701 (2006).
- [6] Holme, P. & Saramäki, J. Temporal networks, *Phys. Rep.* **519**, 97-125 (2012).
- [7] Zanette, D. H. Dynamics of rumor propagation on small-world networks. *Phys. Rev. E* **65**, 041908 (2002).
- [8] Liu, Z., Lai, Y. C., & Ye, N. Propagation and immunization of infection on general networks with both homogeneous and heterogeneous components. *Phys. Rev. E* **67**, 031911 (2003).
- [9] Noh, J. D., & Rieger, H. Random Walks on Complex Networks. *Phys. Rev. Lett.* **92**, 118701 (2004).
- [10] Zhou, J., Liu, Z. & Li, B. Influence of network structure on rumor propagation. *Phys. Lett. A* **368**, 458 (2007).
- [11] Funk, S., Salathé, M. & Jansen, V. A. A. Modelling the influence of human behaviour on the spread of infectious diseases: a review. *J. R. Soc. Interface* **7**, 1257-1274 (2010).
- [12] Meloni, S., Perra, N., Arenas, A., Gómez, S., Moreno, Y. & Vespignani, A. Modeling human mobility responses to the large-scale spreading of infectious diseases. *Sci. Rep.* **1**, 62 (2011).
- [13] Wang, B., Cao, L., Suzuki, H. & Aihara, K. Safety-information-driven human mobility patterns with metapopulation epidemic dynamics, *Sci. Rep.* **2**, 887 (2012).
- [14] Tai, Z. & Sun, T. Media dependencies in a changing media environment: The case of the 2003 SARS epidemic in China. *New. Media. Soc.* **9**, 987-1010 (2007).
- [15] Manfredi, P. & D'Onofrio, A. *Modeling the Interplay Between Human Behavior and the Spread of Infectious Diseases* (Springer-Verlag, Berlin, 2013).
- [16] Funk, S., Gilada, E., Watkins, C., & Jansen, V. A. A. The spread of awareness and its impact on epidemic outbreaks. *Proc. Natl. Acad. Sci.* **106**, 6872 (2009).
- [17] Funk, S., Gilad, E. & Jansen, V. A. A. Endemic disease, awareness, and local behavioural response. *J. Theor. Biol.* **264**, 501-509(2010).
- [18] Funk, S. & Jansen, V. A. A. Interacting epidemics on overlay networks. *Phys. Rev. E* **81**, 036118 (2010).
- [19] Marceau, V., Noël, P. A., Hébert-Dufresne, L., Allard, A. & Dubé, L. J. Modeling the dynamical interaction between epidemics on overlay networks. *Phys. Rev. E* **84**, 026105 (2011).
- [20] Karrer, B. & Newman, M. E. J. Competing epidemics on complex networks. *Phys. Rev. E* **84**, 036106 (2011).
- [21] Ahn, Y. -Y., Jeong, H., Masuda, N. & Noh, J. D. Epidemic dynamics of two species of interacting particles on scale-free networks. *Phys. Rev. E* **74**, 066113 (2006).

- [22] Kiss, I. Z., Cassell, J., Recker, M., & Simon, P. L. The impact of information transmission on epidemic outbreaks. *Math. Biosci.* **225**, 1-10 (2010).
- [23] Perra, N., Balcan, D., Gonçalves, B. & Vespignani, A. Towards a Characterization of Behavior-Disease Models. *PLoS ONE* **6**, e23084 (2011).
- [24] Sahneh, F. D., Chowdhury, F. N., & Scoglio, C. M. On the existence of a threshold for preventive behavioral responses to suppress epidemic spreading. *Sci. Rep.* **2**, 632 (2012).
- [25] Wu, Q., Fu, X., Small, M., & Xu, X. J. The impact of awareness on epidemic spreading in networks. *Chaos* **22**, 013101 (2012).
- [26] Ruan, Z., Tang, M. & Liu, Z. Epidemic spreading with information-driven vaccination. *Phys. Rev. E* **86**, 036117 (2012).
- [27] Jo, H.-H., Baek, S.K. & Moon, H.-T. Immunization dynamics on a two-layer network model. *Physica A* **361**, 534-542 (2006).
- [28] Wang, B., Cao, L., Suzuki, H. & Aihara, K. Impacts of clustering on interacting epidemics. *J. Theor. Biol.*, **304**, 121-130 (2012).
- [29] Jiang, Z. Q., Xie, W. J., Li, M. X., Podobnik, B., Zhou, W. X. & Stanley, H. E. Calling patterns in human communication dynamics. *Proc. Natl. Acad. Sci.* **110**, 1600 (2013).
- [30] Faloutsos, M., Faloutsos, P., & Faloutsos, C. On power-law relationships of the Internet topology. *Comput. Commun. Rev.* **29**, 251 (1999).
- [31] Starnini, M., Baronchelli, A. & Pastor-Satorras, R. Modeling Human Dynamics of Face-to-Face Interaction Networks. *Phys. Rev. Lett.* **110**, 168701 (2013).
- [32] Buldyrev, S. V., Parshani, R., Paul, G., Stanley, H. E. & Havlin, S. Catastrophic cascade of failures in interdependent Networks. *Nature (London)* **464**, 1025 (2010).
- [33] Gao, J., Buldyrev, S. V., Stanley, H. E. & Havlin, S. Networks formed from interdependent networks. *Nat. Phys.* **8**, 40-48 (2012).
- [34] Cozzo, E., Baños, R. A., Meloni, S. & Moreno, Y. Contact-based social contagion in multiplex networks. *Phys. Rev. E* **88**, 050801(R) (2013).
- [35] Kivelä, M., Arenas, A., Barthelemy, M., Gleeson, J. P., Moreno, Y. & Porter, M. A. Multilayer Networks. arXiv:1309.7233v1 (2013).
- [36] Kim, J. Y & Goh, K.-I. Coevolution and Correlated Multiplexity in Multiplex Networks. *Phys. Rev. Lett.* **111**, 058702 (2013).
- [37] Parshani, R., Rozenblat, C., Ietri, D., Ducruet, C., & Havlin, S. Inter-similarity between coupled networks. *Europhys. Lett.* **92**, 68002 (2010).
- [38] Shao, J., Buldyrev, S. V., Havlin, S. & Stanley, H. E. Cascade of failures in coupled network systems with multiple support-dependence relations. *Phys. Rev. E* **83**, 036116 (2011).
- [39] Lee, K.-M., Kim, J. Y., Cho, W. -K., Goh, K. -I. & Kim, I. -M. Correlated multiplexity and connectivity of multiplex random networks. *New J. Phys.* **14**, 033027 (2012).
- [40] Mills, H. L., Ganesh, A. & Colijn, C. Pathogen spread on coupled networks: effect of host and network properties on transmission thresholds. *J. Theor. Biol.* **320**, 47 (2013).
- [41] Gómez, S., Díaz-Guilera, A., Gómez-Gardeñes, J., Pérez-Vicente, C. J., Moreno, Y. & Arenas, A. Diffusion Dynamics on Multiplex Networks. *Phys. Rev. Lett.* **110**, 028701 (2013).
- [42] Cho, W.-K., Goh, K.-I. & Kim, I.-M. Correlated couplings and robustness of coupled networks. arXiv:1010.4971 (2010).
- [43] Moreno, Y., Pastor-Satorras, R. & Vespignani, A. Epidemic outbreaks in complex heterogeneous networks. *Eur. Phys. J. B* **26**, 521-529 (2002).
- [44] Barthélemy, M., Barrat, A., Pastor-Satorras, R. & Vespignani, A. Velocity and Hierarchical Spread of Epidemic Outbreaks in Scale-Free Networks. *Phys. Rev. Lett.* **92**, 178701 (2004).
- [45] Newman, M. E. J. Threshold Effects for Two Pathogens Spreading on a Network. *Phys. Rev. Lett.* **95**, 108701 (2005).
- [46] Newman, M. E. J. Power laws, Pareto distributions and Zipf's law. *Contemp. Phys.* **46**, 323-351 (2005).
- [47] Catanzaro, M., Boguñá, M. & Pastor-Satorras, R. Generation of uncorrelated random scale-free networks. *Phys. Rev. E* **71**, 027103 (2005).
- [48] Newman, M. E. J., Strogatz, S. H. & Watts, D. J. Random graphs with arbitrary degree distributions and their applications. *Phys. Rev. E* **64**, 026118 (2001).
- [49] Erdős, P. & Rényi, On random graphs. *Publ. Math.* **6**, 290-297 (1959).
- [50] Marro, J. & Dickman, R. *Nonequilibrium Phase Transitions in Lattice Models* (Cambridge University Press, Cambridge, 1999).
- [51] Hong, H., Ha, M. & Park, H. Finite-Size Scaling in Complex Networks. *Phys. Rev. Lett.* **98**, 258701 (2007).
- [52] Ferreira, S. C., Castellano, C. & Pastor-Satorras, R. Epidemic thresholds of the susceptible-infected-susceptible model on networks: A comparison of numerical and theoretical results. *Phys. Rev. E* **86**, 041125 (2012).
- [53] Boguñá, M., Castellano, C. & Pastor-Satorras, R. Nature of the epidemic threshold for the susceptible-infected-susceptible dynamics in networks. *Phys. Rev. Lett.* **111**, 068701 (2013).
- [54] Szell, M., Lambiotte, R. & Thurner, S. Multirelational Organization of Large-scale Social Networks in an Online World. *Proc. Natl. Acad. Sci.* **107**, 13636 (2010).
- [55] Nicosia, V., Bianconi, G., Latora, V. & Barthelemy, M. Growing Multiplex Networks. *Phys. Rev. Lett.* **111**, 058701 (2013).
- [56] Holme, P., Kim, B. J., Yoon, C. N. & Han, S. K. Attack vulnerability of complex networks. *Phys. Rev. E* **65**, 056109 (2002).
- [57] Bauch, C. T., & Galvani, A. P. Social Factors in Epidemiology. *Science* **342**, 4 (2013).
- [58] C. Granell, S. Gómez, and A. Arenas. Dynamical interplay between awareness and epidemic spreading in multiplex networks. *Phys. Rev. Lett.* **111**, 128701 (2013).
- [59] Newman, M. E. J. *Networks An Introduction* (Oxford University Press, Oxford, 2010).

Figure legends

FIG 1: Illustration of asymmetrically coupled spreading processes on a simulated communication-contact double-layer net-

work. (a) Communication and contact networks, denoted as layer A and layer B , respectively, each of five nodes. (b) At $t = 0$, node B_1 in layer B is randomly selected as the initial infected node and its counterpart, node A_1 in layer A , gains the information that B_1 is infected, while all other pairs of nodes, one from layer A and another from layer B , are in the susceptible state. (c) At $t = 1$, within layer A the information is transmitted from A_1 to A_2 with probability β_A . Node B_3 in layer B can be infected by node B_1 with probability β_B and, if it is indeed infected, its corresponding node A_3 in layer A gets the information as well. Since, by this time, A_2 is already aware of the infection spreading, its counterpart B_2 in layer B is vaccinated, say with probability p . At the same time, node A_1 in layer A and its counterpart B_1 in layer B enter into the refractory state with probability μ_A and μ_B , respectively. (d) At $t = 2$, all infected nodes in both layers can no longer infect others, and start recovering from the infection. In both layers, the spreading dynamics terminate by this time.

FIG 2: On SF-ER networks, (a) the susceptibility measure χ as a function of the information-transmission rate β_A for $p = 0.5$, $\beta_B = 0.0$ (red squares) and $\beta_B = 0.1$ (green circles), (b) the threshold β_{Ac} of information spreading as a function of the disease-transmission rate β_B for vaccination rate $p = 0.5$ (red squares) and $p = 0.9$ (green circles), where the red solid lines are analytical predictions from Eq. (9).

FIG 3: For SF-ER double-layer networks, epidemic threshold β_{Bc} as a function of the information-transmission rate β_A (a) and the vaccination rate p (b). In (a), the red solid ($p = 0.5$) and green dashed ($p = 0.9$) lines are the analytical predictions from Eq. (11), and the blue dot-dashed line denotes the case of $\theta = 1$ from Eq. (10). The inset of (a) shows the condition under which a giant residual cluster of layer B exists [from Eq. (S20) in Supporting Information] in phase I. In (b), the red solid line ($\beta_A = 0.05$) corresponds to $\beta_{Bc} = \beta_{Bu}$, and the green dashed line ($\beta_A = 0.20$) is the analytical prediction from Eq. (11).

FIG 4: For SF-ER networks, the final density in each state versus the parameters β_A and β_B : (a) recovered density R_A , (b) recovered density R_B , (c) the vaccination density V_B , and (d) V_B versus β_B for $\beta_A = 0.2, 0.5, 0.9$. The value of parameter p is 0.5. Different lines are the numerical solutions of Eqs. (1)-(8) in the limit $t \rightarrow \infty$. In (a) and (d), we select three different values of β_A (0.2, 0.5, and 0.9), corresponding to the red solid, green dashed, and blue dot-dashed lines, respectively. In (b) and (c), three different values of β_B are chosen (0.2, 0.5, and 0.9), corresponding to the red solid, green dashed, and blue dot-dashed lines, respectively.

FIG 5: For two-layer correlated networks with vaccination probability $p = 0.5$, the effect of one type of spreading dynamics on the outbreak threshold of the counter-type spreading dynamics. (a) β_{Ac} versus β_B on SF-ER networks with $q = 0.0$ (red squares) and $q = 0.8$ (green circles), and ER-ER networks with $q = 0.0$ (blue up triangles) and $q = 0.8$ (orange down triangles). Red solid (SF-ER) and blue dashed (ER-ER) lines are the analytical predictions from Eq. (9) and Eq. (S37) (in Supporting Information), respectively. The inset shows the inter-layer correlation m_s as a function of rematching probability q . (b) β_{Bc} versus β_A on SF-ER networks with $q = 0.0$ (red squares) and $q = 0.8$ (green circles), and ER-ER networks with $q = 0.0$ (blue up triangles) and $q = 0.8$ (orange down triangles). Blue solid ($q = 0.0$) and orange dashed ($q = 0.8$) lines are the analytical predictions for ER-ER networks from Eqs. (S38)-(S41) in Supporting Information.

FIG 6: Effect of varying the rematching probability on outbreak thresholds of the two types of spreading dynamics. (a) β_{Ac} versus q on SF-ER (red squares) and ER-ER networks (green circles) for $\beta_B = 0.05$ and $p = 0.5$. Red Solid (SF-ER) and green dashed (ER-ER) lines are analytical predictions from Eq. (9) and Eq. (S37) in Supporting Information, respectively. (b) β_{Bc} versus q on SF-ER (red squares) and ER-ER networks (green circles) for $\beta_A = 0.2$ and $p = 0.5$. Green solid line is analytical prediction for ER-ER networks from Eqs. (S38)-(S41) in Supporting Information.

FIG 7: Effect of rematching probability on the final state. (a) R_A versus q on SF-ER (red squares) and ER-ER networks (blue up triangles), R_B versus q on SF-ER (green circles) and ER-ER networks (orange down triangles). (b) V_B versus q on SF-ER (red squares) and ER-ER networks (green circles). Different lines represent the analytic solutions for ER-ER networks, calculated by summing the final densities of all degrees from Eqs. (S28)-(S34) in Supporting Information. The parameter setting is $\beta_A = 0.2$, $\beta_B = 0.4$ and $p = 0.5$.

Acknowledgement

M.T. would like to thank Prof. Pakming Hui for stimulating discussions. This work was partially supported by the National Natural Science Foundation of China (Grant No. 11105025) and China Postdoctoral Science Special Foundation (Grant No. 2012T50711). Y. Do was supported by Basic Science Research Program through the National Research Foundation of Korea (NRF) funded by the Ministry of Education, Science and Technology (NRF-2013R1A1A2010067). Y.C.L. was supported by AFOSR under Grant No. FA9550-10-1-0083. GW Lee was supported by the Korea Meteorological Administration Research and Development Program under Grant CATER 2012-2072.

Author contributions

W. W., M. T. and Y. C. L devised the research project. W. W. and H. Y. performed numerical simulations. W. W., M. T., Y. H. D. and Y. C. L analyzed the results. W. W., M. T., Y. H. D., Y. C. L and GW. L wrote the paper.

Additional information

Competing financial interests: The authors declare no competing financial interests.

S1. Spreading dynamics on uncorrelated double-layer networks

We adopt the heterogeneous mean-field theory [1] to uncorrelated double-layer networks. Let $P_A(k_A)$ and $P_B(k_B)$ be the degree distributions of layers A and B , with mean degree $\langle k_A \rangle$ and $\langle k_B \rangle$, respectively. We assume that the subnetworks associated with both layers are random with no degree correlation. The time evolution of the epidemic spreading is described by the variables $s_{k_A}^A(t)$, $\rho_{k_A}^A(t)$, and $r_{k_A}^A(t)$, which are the densities of the susceptible, infected, and recovered nodes of degree k_A in layer A at time t , respectively. Similarly, $s_{k_B}^B(t)$, $\rho_{k_B}^B(t)$, $r_{k_B}^B(t)$, and $v_{k_B}^B(t)$ respectively denote the susceptible, infected, recovered, and vaccinated densities of nodes of degree k_B in layer B at time t .

A. Mean-field rate equations

The mean-field rate equations of the information spreading in layer A are then

$$\frac{ds_{k_A}^A(t)}{dt} = -s_{k_A}^A(t)[\beta_A k_A \Theta_A(t) + \beta_B \Theta_B(t) \sum_{k_B} k_B P_B(k_B)], \quad (\text{S1})$$

$$\frac{d\rho_{k_A}^A(t)}{dt} = s_{k_A}^A(t)[\beta_A k_A \Theta_A(t) + \beta_B \Theta_B(t) \sum_{k_B} k_B P_B(k_B)] - \rho_{k_A}^A(t), \quad (\text{S2})$$

$$\frac{dr_{k_A}^A(t)}{dt} = \rho_{k_A}^A(t). \quad (\text{S3})$$

The mean-field rate equations of epidemic spreading in layer B are thus given by

$$\frac{ds_{k_B}^B(t)}{dt} = -s_{k_B}^B(t)\beta_B k_B \Theta_B(t) - p\beta_A \Theta_A(t) \sum_{k_A} s_{k_A}^A(t)k_A P_A(k_A), \quad (\text{S4})$$

$$\frac{d\rho_{k_B}^B(t)}{dt} = s_{k_B}^B(t)\beta_B k_B \Theta_B(t) - \rho_{k_B}^B(t), \quad (\text{S5})$$

$$\frac{dr_{k_B}^B(t)}{dt} = \rho_{k_B}^B(t), \quad (\text{S6})$$

$$\frac{dv_{k_B}^B(t)}{dt} = p\beta_A \Theta_A(t) \sum_{k_A} s_{k_A}^A(t)k_A P_A(k_A), \quad (\text{S7})$$

where $\Theta_A(t)$ [$\Theta_B(t)$] is the probability that a neighboring node in layer A (layer B) is in the infected state.

From Eqs. (S1)-(S7), the density associated with each distinct state in layer A or B is given by

$$X_h(t) = \sum_{k_h=1}^{k_{h,max}} P_h(k_h) X_{k_h}^h(t). \quad (\text{S8})$$

where $h \in \{A, B\}$, $X \in \{S, I, R, V\}$, and $k_{h,max}$ denotes the largest degree of layer h . The final densities of the whole system can be obtained by taking the limit $t \rightarrow \infty$.

B. Linear analysis for the information threshold

On an uncorrelated layered network, at the outset of the spreading dynamics, the whole system can be regarded as consisting of two coupled SI-epidemic subsystems [2] with the time evolution described by Eqs. (S2) and (S5). For $t \rightarrow 0$, we have $s_{k_A}^A(t) \approx 1$ and $s_{k_B}^B(t) \approx 1$, which reduce Eqs. (S2) and (S5) to

$$\begin{cases} \frac{d\rho_{k_A}^A(t)}{dt} = \beta_A k_A \Theta_A(t) + \beta_B \langle k_B \rangle \Theta_B(t) - \rho_{k_A}^A(t), \\ \frac{d\rho_{k_B}^B(t)}{dt} = \beta_B k_B \Theta_B(t) - \rho_{k_B}^B(t). \end{cases} \quad (\text{S9})$$

For convenience, Eq. (S9) can be written concisely as

$$\frac{d\vec{\rho}}{dt} = C\vec{\rho} - \vec{\rho}, \quad (\text{S10})$$

where the vector of infected density is defined as

$$\vec{\rho} \equiv (\rho_{k_A=1}^A, \dots, \rho_{k_A, \max}^A, \rho_{k_B=1}^B, \dots, \rho_{k_B, \max}^B)^T,$$

and C is a block matrix in the following form:

$$C = \begin{pmatrix} C^A & D^B \\ 0 & C^B \end{pmatrix}, \quad (\text{S11})$$

with matrix elements given by

$$\begin{aligned} C_{k_A, k'_A}^A &= [\beta_A k_A (k'_A - 1) P_A(k'_A)] / \langle k_A \rangle, \\ C_{k_B, k'_B}^B &= [\beta_B k_B (k'_B - 1) P_B(k'_B)] / \langle k_B \rangle, \\ D_{k_B, k'_B}^B &= \beta_B (k'_B - 1) P_B(k'_B). \end{aligned}$$

In general, information spreading on layer A can be facilitated by the outbreak of the epidemic on layer B , as an infected node in layer B instantaneously makes its counterpart node in layer A “infected” with the information about the disease. This coupling effect, in combination with the intrinsic spreading dynamics on layer A , leads to more informed nodes in the communication layer than infected nodes on layer B . If the maximum eigenvalue Λ_C of matrix C is greater than 1, an outbreak of the information will occur in the system [3]. We then have

$$\Lambda_C = \max\{\Lambda_A, \Lambda_B\}, \quad (\text{S12})$$

where $\max\{\}$ denotes the greater of the two, and

$$\begin{aligned} \Lambda_A &= \beta_A (\langle k_A^2 \rangle - \langle k_A \rangle) / \langle k_A \rangle, \\ \Lambda_B &= \beta_B (\langle k_B^2 \rangle - \langle k_B \rangle) / \langle k_B \rangle \end{aligned}$$

are the maximum eigenvalues of matrices C^A and C^B [4], respectively. The outbreak threshold of information spreading in layer A is given by

$$\beta_{Ac} = \begin{cases} \beta_{Au}, & \text{for } \beta_B \leq \beta_{Bu} \\ 0, & \text{for } \beta_B > \beta_{Bu} \end{cases} \quad (\text{S13})$$

where $\beta_{Au} \equiv \langle k_A \rangle / (\langle k_A^2 \rangle - \langle k_A \rangle)$ and $\beta_{Bu} \equiv \langle k_B \rangle / (\langle k_B^2 \rangle - \langle k_B \rangle)$ denote the outbreak threshold of information spreading on layer A when it is isolated from layer B , and that of epidemic spreading on layer B when the coupling between the two layers is absent, respectively.

C. Competing percolation theory for epidemic threshold

To elucidate the interplay between epidemic and vaccination spreading, we must first determine which one is the faster “disease.” At the early time of the epidemic outbreak on the isolated layer B , the average number of infected nodes grows exponentially as

$$N_e = n_0 R_e^t = n_0 e^{t \ln R_e}, \quad (\text{S14})$$

where $R_e = \beta_B/\beta_{Bu}$ is the basic reproductive number for the disease on the isolated layer B [5], and n_0 denotes the number of initially infected nodes. Similarly, for information spreading on the isolated layer A , the average number of informed nodes at the early time is

$$N_i = n_0 R_i^t = n_0 e^{t \ln R_i}, \quad (\text{S15})$$

where $R_i = \beta_A/\beta_{Au}$ is the reproductive number for information spreading on the isolated layer A . The resulting number of vaccinated nodes on layer B is

$$N_v = p n_0 R_i^t = p n_0 e^{t \ln R_i}. \quad (\text{S16})$$

Since both epidemic and vaccination spreading processes exhibit exponential growth, we can obtain the ratio of their growth rates as

$$\theta = \frac{R_e}{R_i} = \frac{\beta_B \beta_{Au}}{\beta_A \beta_{Bu}}. \quad (\text{S17})$$

For $\theta > 1$, i.e., $\beta_B \beta_{Au} > \beta_A \beta_{Bu}$, the epidemic disease spreads faster than the vaccination. In this case, the vaccination spread is insignificant and can be neglected.

To uncover the impact of information spreading on epidemic outbreak, we focus on the case of faster vaccination, i.e., $\theta < 1$, in accordance with the fact that information always tends to spread much faster than epidemic in a modern society. Given that vaccination and epidemic can be treated successively and separately, the threshold of epidemic outbreak can be derived by a bond percolation analysis [6, 7].

Firstly, when information spreading on layer A is over, the density of informed population is given by [5]

$$S_A = 1 - G_{A0}(u), \quad (\text{S18})$$

where $G_{A0}(x) = \sum_{k_A} P_A(k_A) x^{k_A}$ is the generating function for the degree distribution of layer A , and u is the probability that a node is not connected to the giant cluster via a particular one of its edges, which can be solved by

$$u = 1 - \beta_A + \beta_A G_{A1}(u), \quad (\text{S19})$$

where $G_{A1}(x) = \sum_{k_A} Q_A(k_A) x^{k_A}$ is the generating function for the excess degree distribution, $Q_A(k_A) = (k_A + 1)P_A(k_A + 1)/\langle k_A \rangle$, of layer A . Since p is the probability that an informed node in layer A makes its counterpart node in layer B vaccinated, the number of vaccinated or removed nodes in layer B is pS_A . A necessary condition for the outbreak of epidemic is the existence of a giant residual cluster in layer B [8]. We have

$$1 - pS_A > f_{Bc} = \frac{1}{G'_{B1}(1)}, \quad (\text{S20})$$

where $G_{B1}(x) = \sum_{k_B} Q_B(k_B) x^{k_B}$ is the generating function for the excess degree distribution, $Q_B(k_B) = (k_B + 1)P_B(k_B + 1)/\langle k_B \rangle$, of layer B , and the prime denotes derivative. From Eq. (S20), we see that epidemic outbreak can occur only if $pS_A < 1 - 1/G'_{B1}(1)$.

The degree distribution of the residual network of layer B is given by [9, 10]

$$\tilde{P}_B(\tilde{k}_B) = f \sum_{k'_B=\tilde{k}_B}^{\infty} P_B(k'_B) \binom{k'_B}{\tilde{k}_B} (1-f)^{k'_B-\tilde{k}_B} f^{\tilde{k}_B}, \quad (\text{S21})$$

where $f = 1 - pS_A$ is the probability that a node is in the residual network. The generating function for the degree distribution of the residual network is then [6]

$$H_{B0}(x) = f G_{B0}(1 - f + fx), \quad (\text{S22})$$

where $G_{B0}(x) = \sum_{k_B} P_B(k_B) x^{k_B}$ is the generating function for the degree distribution of layer B . The generating function for its excess degree distribution is

$$H_{B1}(x) = \frac{H'_{B0}(x)}{H'_{B0}(1)}. \quad (\text{S23})$$

The basic reproductive number for a disease spreading over the residual network of layer B is then given by [5]

$$\tilde{R}_i = \beta_B H'_{B1}(1). \quad (\text{S24})$$

The epidemic threshold corresponds to the point $\tilde{R}_i = 1$, and thus we have $\beta_{Bc} = 1/H'_{B1}(1)$. From Eqs. (S22)-(S24), we obtain the epidemic threshold β_{Bc} as

$$\beta_{Bc} = \frac{\langle k_B \rangle}{(1 - pS_A)(\langle k_B^2 \rangle - \langle k_B \rangle)}, \quad (\text{S25})$$

where S_A is the density of the informed population, which can be obtained by solving Eqs. (S18) and (S19).

S2. Spreading dynamics on correlated double-layer networks

We assume that layer A has the same degree distribution as layer B . After a certain fraction q of pairs of nodes, one from each layer, have been randomly rematched, the conditional probability $P(k_B|k_A)$ can be written as

$$P(k_B|k_A) = qP_B(k_B) + (1-q)\delta_{k_B,k_A}, \quad (\text{S26})$$

or

$$P(k_A|k_B) = qP_A(k_A) + (1-q)\delta_{k_A,k_B}. \quad (\text{S27})$$

A. Mean-field rate equations

Using Eqs. (S1)-(S3), we can write the mean-field rate equations for information spreading on layer A as

$$\frac{ds_{k_A}^A(t)}{dt} = -s_{k_A}^A(t)\{\beta_A k_A \Theta_A(t) + \beta_B \Theta_B(t) \sum_{k_B} k_B [qP_B(k_B) + (1-q)\delta_{k_B,k_A}]\}, \quad (\text{S28})$$

$$\frac{d\rho_{k_A}^A(t)}{dt} = s_{k_A}^A(t)\{\beta_A k_A \Theta_A(t) + \beta_B \Theta_B(t) \sum_{k_B} k_B [qP_B(k_B) + (1-q)\delta_{k_B,k_A}]\} - \rho_{k_A}^A(t), \quad (\text{S29})$$

$$\frac{dr_{k_A}^A(t)}{dt} = \rho_{k_A}^A(t). \quad (\text{S30})$$

Similarly, the mean-field rate equations for epidemic spreading on layer B are

$$\frac{ds_{k_B}^B(t)}{dt} = -s_{k_B}^B(t)\beta_B k_B \Theta_B(t) - p\beta_A \Theta_A(t) \sum_{k_A} s_{k_A}^A(t) k_A [qP_A(k_A) + (1-q)\delta_{k_A,k_B}], \quad (\text{S31})$$

$$\frac{d\rho_{k_B}^B(t)}{dt} = s_{k_B}^B(t)\beta_B k_B \Theta_B(t) - \rho_{k_B}^B(t), \quad (\text{S32})$$

$$\frac{dr_{k_B}^B(t)}{dt} = \rho_{k_B}^B(t), \quad (\text{S33})$$

$$\frac{dv_{k_B}^B(t)}{dt} = p\beta_A \Theta_A(t) \sum_{k_A} s_{k_A}^A(t) k_A [qP_A(k_A) + (1-q)\delta_{k_A,k_B}]. \quad (\text{S34})$$

Substituting Eqs. (S28)-(S34) into Eq. (S8), we can get the density associated with each distinct state in layer A or B .

B. Linear analysis for the information threshold

At the outset of the spreading dynamics, the whole system can be regarded as two coupled SI-epidemic subsystems [2] with the time evolution described by Eqs. (S29) and (S32). In the limit $t \rightarrow 0$, we have $s_{k_A}^A(t) \approx 1$ and $s_{k_B}^B(t) \approx 1$. Equations (S29) and (S32) can then be reduced to

$$\begin{cases} \frac{d\rho_{k_A}^A(t)}{dt} = \beta_A k_A \Theta_A(t) + \beta_B [q\langle k_B \rangle + (1-q)k_A] \Theta_B(t) - \rho_{k_A}^A(t), \\ \frac{d\rho_{k_B}^B(t)}{dt} = \beta_B k_B \Theta_B(t) - \rho_{k_B}^B(t). \end{cases} \quad (\text{S35})$$

which can be written concisely as

$$\frac{d\vec{\rho}}{dt} = C\vec{\rho} - \vec{\rho}, \quad (\text{S36})$$

where the matrix C has the same form as in Eq. (S11) and

$$\begin{aligned} C_{k_A, k'_A}^A &= [\beta_A k_A (k'_A - 1) P_A(k'_A)] / \langle k_A \rangle, \\ C_{k_B, k'_B}^B &= [\beta_B k_B (k'_B - 1) P_B(k'_B)] / \langle k_B \rangle, \\ D_{k_B, k'_B}^B &= \beta_B [q \langle k_B \rangle + (1 - q) k_A] (k'_B - 1) P_B(k'_B) / \langle k_B \rangle. \end{aligned}$$

The threshold of information outbreak is given by

$$\beta_{Ac} = \begin{cases} \beta_{Au}, & \text{for } \beta_B \leq \beta_{Bu}, \\ 0, & \text{for } \beta_B > \beta_{Bu}, \end{cases} \quad (\text{S37})$$

which is the same as Eq. (9) in the main text. As described in uncorrelated networks, there are two distinct mechanisms that can lead to the outbreak of information on layer A , and these hold for correlated layered-networks as well. For $\beta_B \leq \beta_{Bu}$, only a small number of nodes in layer B are infected, so the impact of the disease on information-outbreak threshold on layer A is negligible. For $\beta_B > \beta_{Bu}$, epidemic spreading can result in the outbreak of information. In this case, the information-outbreak threshold is zero.

C. Competing percolation theory for epidemic threshold

For $\beta_A \leq \beta_{Au}$, information itself cannot spread through the population. There is thus hardly any effect of the information layer on the epidemic spreading on layer B , and we have $\beta_{Bc} \approx \beta_{Bu}$. But for $\beta_A > \beta_{Au}$, the effect of information spreading on the epidemic threshold cannot be ignored. To assess quantitatively the influence, we focus on the case of faster information spread, i.e., $\beta_A \beta_{Bu} > \beta_B \beta_{Au}$, rendering applicable a bond percolation analysis similar to uncorrelated networks. Specifically, after information spreads on layer A , the percentage of nodes that get the information is S_A , and the density of recovered nodes of degree k_A is $r_{k_A}^A = 1 - u^{k_A}$, where u is the probability that a node is not connected to the giant cluster by a particular edge [Eq. (S19)]. Vaccinating a number of counterpart nodes results in the random removal of some edges which connect the vaccinated nodes with the remaining nodes [9, 10]. The probability \tilde{h} of an edge linking to a vaccinated node is

$$\tilde{h} = \frac{p \sum_{k_B} [(1 - q) r_{k_A} + q S_A] k_B P_B(k_B)}{\langle k_B \rangle}. \quad (\text{S38})$$

The new degree distribution of the residual network on layer B is thus given by

$$\tilde{P}_B(\tilde{k}_B) = \sum_{k'_B = \tilde{k}_B}^{\infty} \{1 - p[(1 - q) r_{k_A} + q S_A]\} P_B(k'_B) \left(\frac{k'_B}{\tilde{k}_B} \right) (1 - \tilde{h})^{\tilde{k}_B} \tilde{h}^{k'_B - \tilde{k}_B}. \quad (\text{S39})$$

The requirement that a giant residual cluster exists is

$$\frac{\langle \tilde{k}_B^2 \rangle}{\langle \tilde{k}_B \rangle} > 2, \quad (\text{S40})$$

where $\langle \tilde{k}_B \rangle$ and $\langle \tilde{k}_B^2 \rangle$ are the first and second moments of the degree distribution, respectively. Finally, we obtain the epidemic threshold as

$$\beta_{Bc} = \frac{\langle \tilde{k}_B \rangle}{\langle \tilde{k}_B^2 \rangle - \langle \tilde{k}_B \rangle}. \quad (\text{S41})$$

S3. Simulation results

We first describe the simulation process of the two spreading dynamics on double-layer networks, and then demonstrate the validity of the theoretical analysis on uncorrelated networks with different network sizes and degree exponents, finally, we present results for SF-SF correlated networks.

A. Simulation process

To initiate an epidemic spreading process, a node in layer B is randomly infected and its counterpart node in layer A is thus in the informed state, too. The updating process is performed with parallel dynamics, which is widely used in statistical physics [11]. At each time step, we first calculate the informed (infected) probability $\pi_A = 1 - (1 - \beta_A)^{n_I^A}$ [$\pi_B = 1 - (1 - \beta_B)^{n_I^B}$] that each susceptible node in layer A (B) may be informed (infected) by its informed (infected) neighbors, where n_I^A (n_I^B) is the number of its informed (infected) neighboring nodes.

According to the dynamic mechanism, once node A_i is in the susceptible state, its counterpart node B_i will be also in the susceptible state. Considering the asymmetric coupling between the two layers in this case, both the information-transmission and disease-transmission events can hardly occur at the same time. Thus, with probability $\pi_A/(\pi_A + \pi_B)$, node A_i have a probability π_A to get the information from its informed neighbors in layer A . If node A_i is informed, its counterpart node B_i will turn into the vaccination state with probability p . With probability $\pi_B/(\pi_A + \pi_B)$, node B_i have a probability π_B to get the infection from its infected neighbors in layer B , and then node A_i also get the information about the disease.

In the other case that node B_i and its corresponding node A_i are in the susceptible state and the informed (or refractory) state respectively, only the disease-transmission event can occur at the time step. Thus, node B_i will be infected with probability π_B .

After renewing the states of susceptible nodes, each informed (infected) node can enter the recovering phase with probability $\mu_A = 1.0$ ($\mu_B = 1.0$). The spreading dynamics terminates when all informed (or infected) nodes in both layers are recovered, and the final densities R_A , R_B , and V_B are then recorded. The simulations are implemented using 30 different two-layer network realizations. The network size of $N_A = N_B = 2 \times 10^4$ and average degrees $\langle k_A \rangle = \langle k_B \rangle = 8$ are used for all subsequent numerical results, unless otherwise specified.

B. Uncorrelated double-layer networks

The effect of network size N on the information and epidemic outbreak thresholds is first studied. According to Eq. (S13), the behavior of the information threshold can be classified into two classes. For $\beta_B \leq \beta_{Bu}$, the disease transmission on layer B has little impact on the information threshold, as we have $\beta_{Ac} \approx \beta_{Au} = \langle k_A \rangle / (\langle k_A^2 \rangle - \langle k_A \rangle)$; while $\beta_{Ac} = 0.0$ for $\beta_B > \beta_{Bu}$. We here focus on the information threshold for $\beta_B \leq \beta_{Bu}$. From Figs. S8(a) and (c), we see that the theoretical predictions are basically accordant with the simulated thresholds for different network sizes. With the growth of network size, the information threshold decreases as $\langle k^2 \rangle$ of layer A increases [12]. According to Eq. (S25), the theoretical epidemic threshold can be predicted. For SF-ER double-layer networks, Figs. S8(b) and (d) shows that the simulated epidemic thresholds deviate slightly from the theoretical predictions. However, the larger deviations occur for the larger values of the vaccination rate p , e.g., $p = 0.9$ in Fig. S9, because the basic assumption of competing percolation theory is not strictly correct for the finite-size networks. As pointed out by Karrer and Newman [7], in the limit of large network size N , the vaccination and epidemic processes can be treated successively and separately. On the double-layer networks with finite network size, the effect of information spreading is somewhat over-emphasized. From Figs. S8 and S9, we also see that the discrepancy between the simulated and theoretical thresholds decreases with network size N .

We then investigate how the degree heterogeneity of layer A influences the information and epidemic outbreak thresholds by adjusting the exponent γ_A . The information thresholds for the different exponents of layer A are compared in Fig. S10(a), and the stronger heterogeneity of layer A (i.e., smaller γ_A) can more easily make the information outbreak. Fig. S10(b) shows that increasing the heterogeneity of layer A can slightly raise the epidemic threshold β_{Bc} at a small information-transmission rate β_A , while making for the epidemic outbreak at a large β_A . This phenomenon results from the different effects of the heterogeneity on the information spreading under different transmission rates. The more homogeneous degree distribution does not always hinder the diffusion of information, especially at a large transmission rate [10, 13].

To further demonstrate the validity of the theoretical analysis, we consider the case of SF-SF double-layer networks. Similar to the case of SF-ER networks, the gap between the theoretical and simulated thresholds is narrowing with the increase of network size [see Figs. S8(d) and S9], which implies the reasonability of the assumption in the thermodynamic limit. The final dynamical state of the SF-SF spreading system is also shown in Fig. S11, and it displays a similar phenomenon to the case of SF-ER networks. We also see that the theoretical predictions from mean-field rate equations are in good agreement with the simulation results.

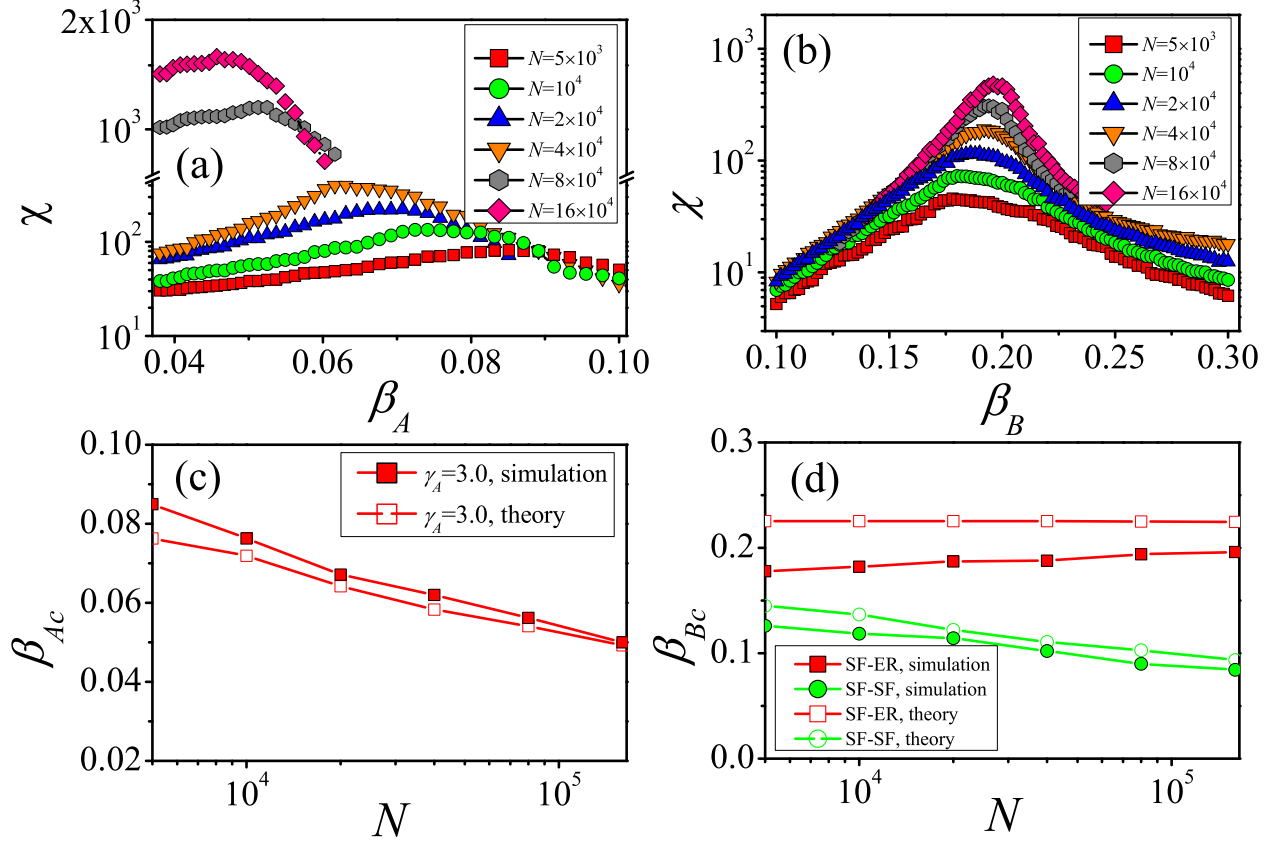


FIG. S 8: (Color online) On SF-ER networks, the susceptibility measure χ as a function of the information-transmission rate β_A at $\beta_B = 0.1$ (a) and the disease-transmission rate β_B at $\beta_A = 0.3$ (b) for $N = 5 \times 10^3$ (red squares), $N = 10^4$ (green circles), $N = 2 \times 10^4$ (blue up triangles), $N = 4 \times 10^4$ (orange down triangles), $N = 8 \times 10^4$ (gray hexagons) and $N = 16 \times 10^4$ (pink diamonds); (c) the information threshold β_{Ac} as a function of network size N at $\beta_B = 0.1$. (d) The epidemic threshold β_{Bc} as a function of N at $\beta_A = 0.3$ for SF-ER networks (red solid squares) and SF-SF networks (green solid circles). The same hollow symbols represent the corresponding theoretical thresholds. The other parameters are the degree exponent $\gamma_A = 3.0$ (or $\gamma_B = 3.0$) and vaccination rate $p = 0.5$.

C. Correlated double-layer networks

On SF-SF correlated networks, we investigate the effect of positive inter-layer correlation on the two types of spreading dynamics. As shown in Figs. S12, S13 and S14, with the increase of the correlation m_s (by reducing the rematching probability q), the information threshold remains unchanged but the epidemic threshold can be enhanced, making the contact layer more robust to epidemic outbreak, which is consistent with the results for ER-ER correlated networks.

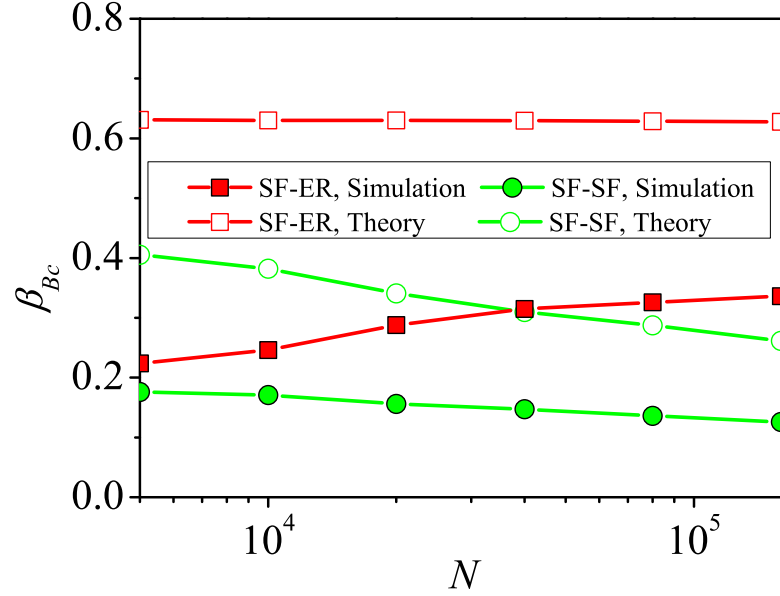


FIG. S 9: (Color online) The epidemic threshold β_{Bc} as a function of network size N for SF-ER networks (red solid squares) and SF-SF networks (green solid circles) at $\beta_A = 0.3$ and $p = 0.9$. The same hollow symbols represent the corresponding theoretical thresholds. For each SF layer, the degree exponent is set to $\gamma_A = 3.0$ (or $\gamma_B = 3.0$).

* Electronic address: tangminghuang521@hotmail.com

- [1] Barthélemy, M., Barrat, A., Pastor-Satorras, R. & Vespignani, A. Velocity and Hierarchical Spread of Epidemic Outbreaks in Scale-Free Networks. *Phys. Rev. Lett.* **92**, 178701 (2004).
- [2] Newman, M. E. J. *Networks An Introduction* (Oxford University Press, Oxford, 2010).
- [3] Saumell-Mendiola, A., Ángeles Serrano, M. & Boguñá, M. Epidemic spreading on interconnected networks. *Phys. Rev. E* **86**, 026106 (2012).
- [4] Mieghe, P. V. *Graph Spectra for Complex Networks* (Cambridge university press, England, 2011).
- [5] Newman, M. E. J. Spread of epidemic disease on networks. *Phys. Rev. E* **66**, 016128 (2002).
- [6] Newman, M. E. J. Threshold Effects for Two Pathogens Spreading on a Network. *Phys. Rev. Lett.* **95**, 108701 (2005).
- [7] Karrer, B. & Newman, M. E. J. Competing epidemics on complex networks. *Phys. Rev. E* **84**, 036106 (2011).
- [8] Gao, J., Buldyrev, S. V., Stanley, H. E. & Havlin, S. Networks formed from interdependent networks. *Nat. Phys.* **8**, 40-48 (2012).
- [9] Cohen, R., Erez, K., ben-Avraham, D., & Havlin, S. Breakdown of the Internet under Intentional Attack. *Phys. Rev. Lett.* **86**, 3682 (2001).
- [10] Pastor-Satorras, R. & Vespignani, A. Immunization of complex networks. *Phys. Rev. E* **65**, 036104 (2002).
- [11] Marro, J. & Dickman, R. *Nonequilibrium Phase Transitions in Lattice Models* (Cambridge University Press, Cambridge, 1999).
- [12] Boguñá, M., Castellano, C. & Pastor-Satorras, R. Nature of the Epidemic Threshold for the Susceptible-Infected-Susceptible Dynamics in Networks. *Phys. Rev. Lett.* **111**, 068701 (2013).
- [13] Pastor-Satorras, R., & Vespignani, A. Epidemic dynamics and endemic states in complex networks. *Phys. Rev. E* **63**, 066117 (2001).

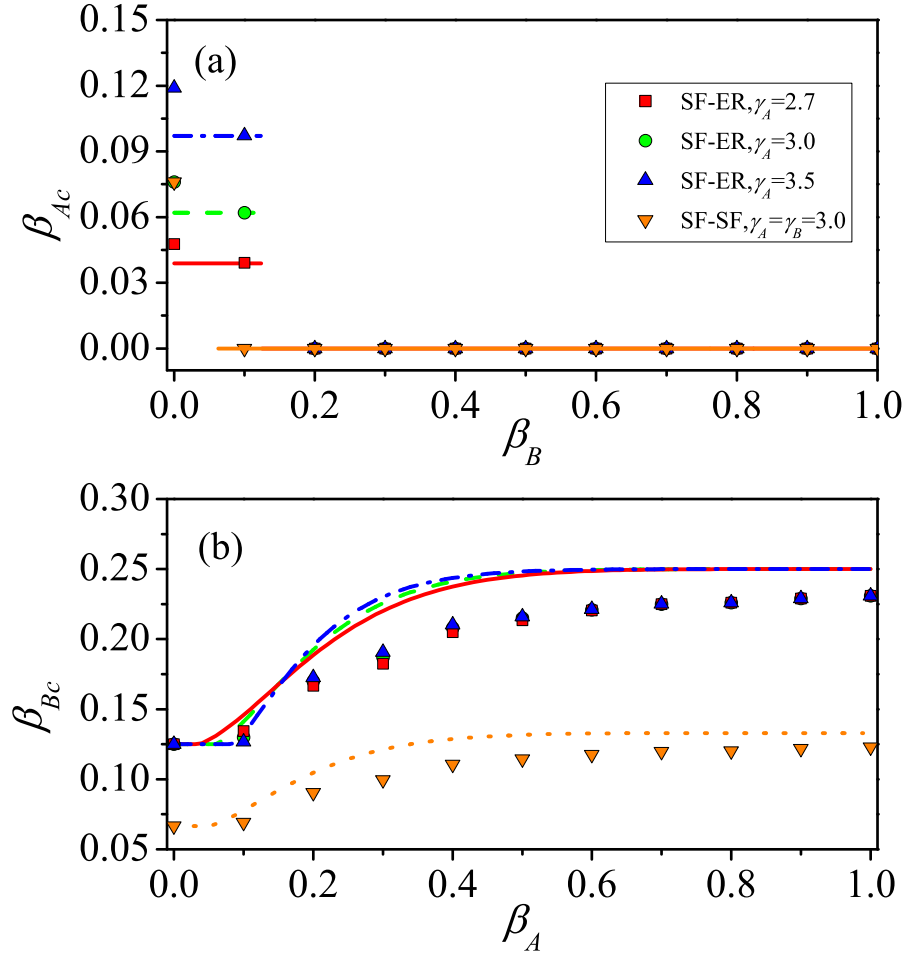


FIG. S 10: (Color online) On various double-layer networks, β_{Ac} versus β_B (a) and β_{Bc} versus β_A (b) for the SF-ER networks with $\gamma_A = 2.7$ (red squares), the SF-ER networks with $\gamma_A = 3.0$ (green circles), the SF-ER networks with $\gamma_A = 3.5$ (blue up triangles) and the SF-SF networks with $\gamma_A = \gamma_B = 3.0$ (orange down triangles). The analytical predictions of β_{Ac} and β_{Bc} are from Eq. (S13) and Eq. (S25), respectively. The vaccination rate is set to $p = 0.5$.

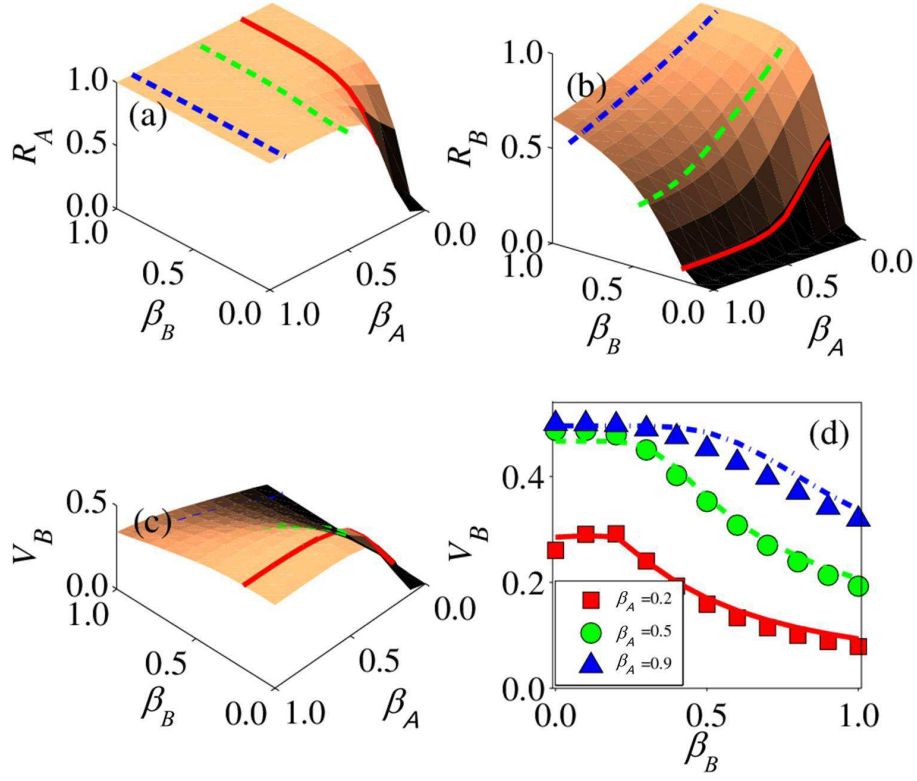


FIG. S 11: (Color online) For SF-SF networks, the final density in each state versus the parameters β_A and β_B : (a) recovered density R_A , (b) recovered density R_B , (c) the vaccination density V_B , and (d) V_B versus β_B for $\beta_A = 0.2, 0.5, 0.9$. The other parameter are $p = 0.5$ and $\gamma_A = \gamma_B = 3.0$. Different lines are the numerical solutions of Eqs. (S1)-(S8) in the limit $t \rightarrow \infty$. In (a) and (d), we select three different values of β_A (0.2, 0.5, and 0.9), corresponding to the red solid, green dashed, and blue dot-dashed lines, respectively. In (b) and (c), three different values of β_B are chosen (0.2, 0.5, and 0.9), corresponding to the red solid, green dashed, and blue dot-dashed lines, respectively.

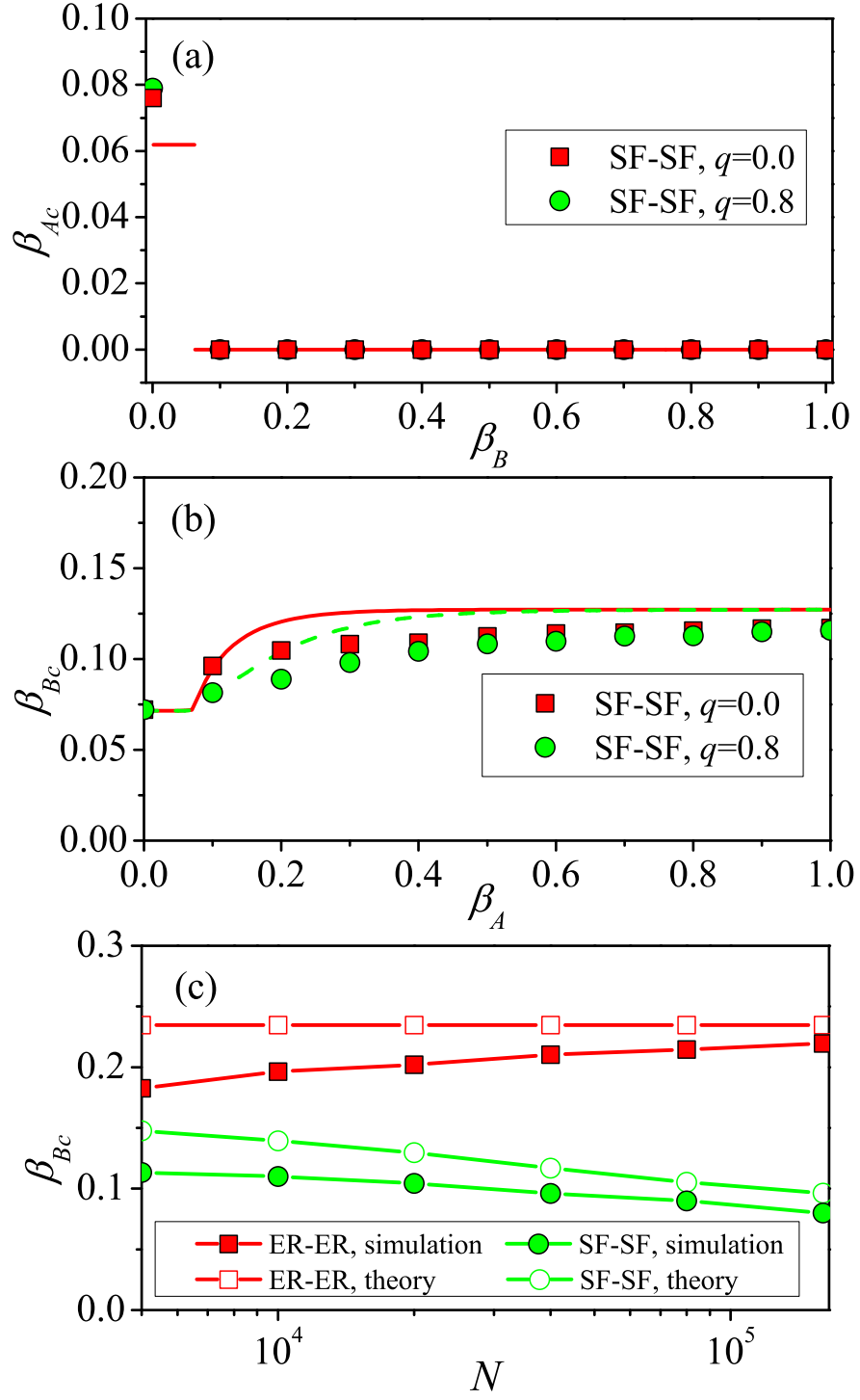


FIG. S 12: (Color online) On double-layer networks, (a) β_{Ac} versus β_B , (b) β_{Bc} versus β_A , and (c) β_{Bc} versus N at $\beta_A = 0.3$. In (a) and (b), red solid squares and green solid circles respectively denote the simulation results for $q = 0.0$ and $q = 0.8$ on SF-SF networks, and the lines are the corresponding theoretical thresholds. In (c), the value of parameter q is 0.0, solid red squares and solid green circles respectively represent the results for ER-ER and SF-SF networks, and the same shapes are the corresponding theoretical predictions. The other parameter are $p = 0.5$ and $\gamma_A = \gamma_B = 3.0$.

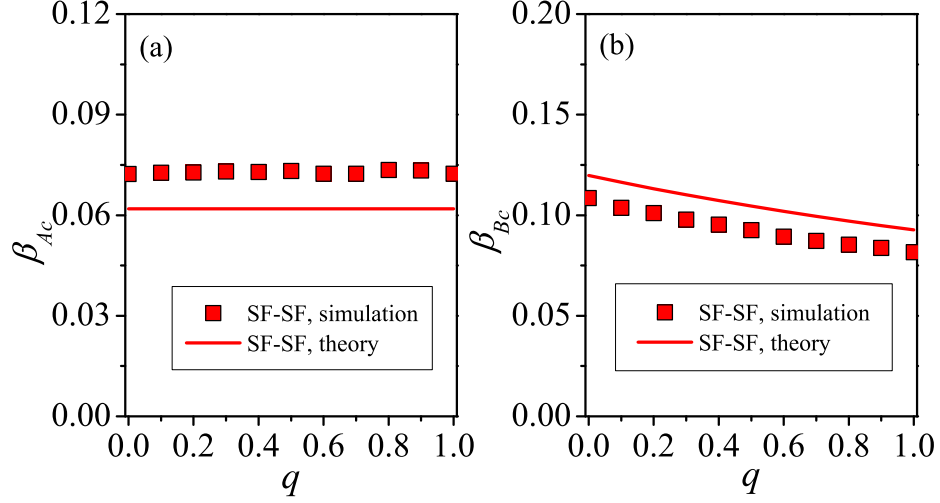


FIG. S 13: (Color online) On SF-SF networks, the effect of varying the rematching probability on outbreak thresholds of the two types of spreading dynamics. (a) β_{Ac} versus q for $\beta_B = 0.05$ and $p = 0.5$. Red Solid line is the analytical prediction from Eq. (S37). (b) β_{Bc} versus q for $\beta_A = 0.2$ and $p = 0.5$. Red solid line is the analytical prediction from Eqs. (S38)-(S41). The value of degree exponent is $\gamma_A = \gamma_B = 3.0$.

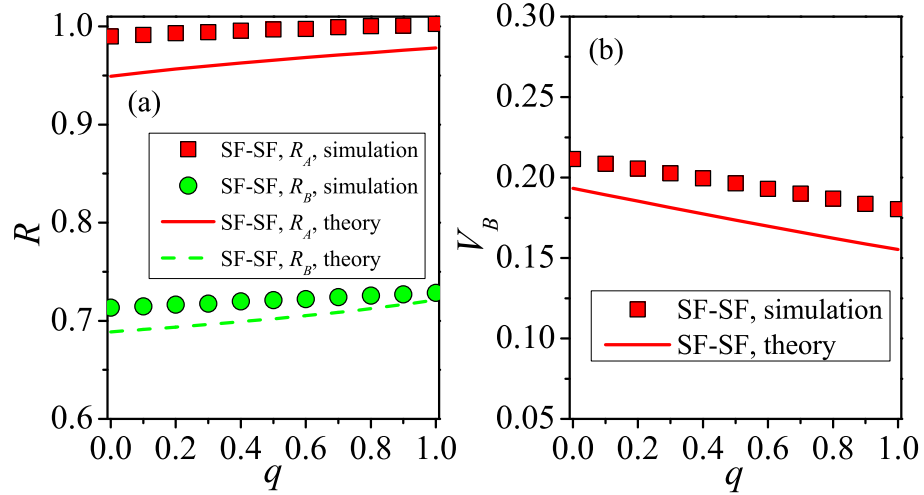


FIG. S 14: (Color online) On SF-SF networks, the effect of rematching probability on the final state. (a) R_A versus q (red squares) and R_B versus q (green circles), (b) V_B versus q (red squares). Different lines represent the analytic solutions for SF-SF networks, calculated by summing the final densities of all degrees from Eqs. (S28)-(S34). The parameter setting is $\gamma_A = \gamma_B = 3.0$, $\beta_A = 0.2$, $\beta_B = 0.4$ and $p = 0.5$.